CENTER *for* MUSCULOSKELETAL RESEARCH

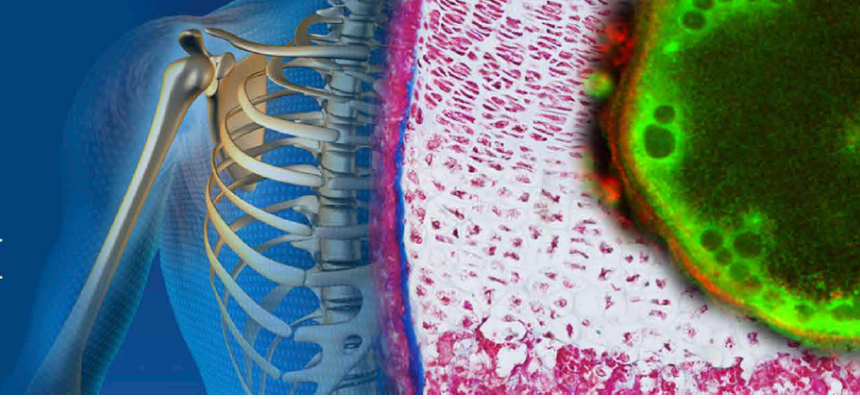

10th Annual CMSR Symposium

Wednesday, November 18, 2020

Sponsored By

Department of Orthopaedics and Rehabilitation
University of Rochester Medical Center
&
National Institute of Arthritis and Musculoskeletal and Skin Diseases (NIAMS) Grant T32 AR076950

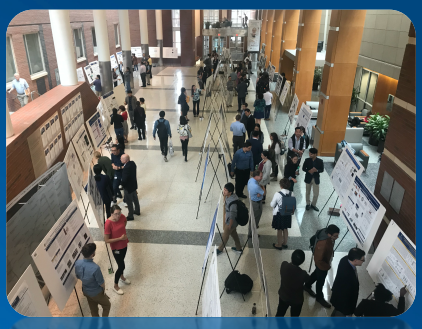

MEDICINE *of* THE HIGHEST ORDER

UR MEDICINE

Center for MusculoSkeletal Research

10th Annual CMSR Symposium

Wednesday, November 18, 2020

Registration Link https://urmc.zoom.us/webinar/register/WN_RqIsqKEOTp-13ZdIFvCtkg

Program

8:30 AM	ePosters Virtual Viewing & Networking	
10:00 AM	Webinar Opening Remarks	Awad, Schwarz, Rubery
10:15 AM	The CMSR: Where We Have Been, Where We Are Going	J Edward Puzas, PhD

Trainees Presentations

Pre-Doc Rosier Awards Finalists

10:45 AM	Investigating Murine Joint-Draining Lymphatics: Lineage Tracing and Single Cell RNA Sequencing Reveal Evidence that Popliteal Lymphatic Muscle Cells and their Progenitors Represent Distinct Cell Types Divergent from Skeletal and Vascular Muscle Cells	Mark Kenney
10:55 AM	The periostin niche as a target for modulating myofibroblast differention to promote regenerative tendon healing	Jessica Ackerman
11:05 AM	Multiphoton microscopy with clearing for three dimensional histology of mouse digital flexor tendon	Melissa MacLiesh
11:15 AM	Semi-Randomized Zwitterionic Peptides Grant Anti-Fouling Behavior to Nanoparticles	Clyde Overby
11:25 AM	NAD(P)H Autofluorescence Lifetime Imaging Enables Single Cell Analyses of Osteoblast Cellular Metabolism	Kevin Schilling
11:35 AM	Age-associated callus senescent cells produce TGF beta1 that inhibits bone fracture healing in aged mice	Jiatong Liu

Post-Doc Rosier Awards Finalists

11:45 AM	IL-27 suppresses Staphylococcal abscess formation in Staphylococcus aureus implant-associated osteomyelitis	Yugo Morita, MD, PhD
11:55 AM	Targeting synovial lymphatic function as a novel therapeutic intervention for osteoarthriti	Xi Lin, PhD
12:05 PM	Targeted radiation evokes catecholamine production triggering rapid inflammatory responses	Yuko Kawano, MD, PhD

New Faculty Spotlight

1:00 PM **Chike Cao, PhD**
Voltage-Gated Calcium Channel CaV1.2 Regulates Heterotopic Ossification in Tendon

1:30 PM **Chia-Lung Wu, PhD**
Application of Next-Generation Sequencing in Musculoskeletal Research: Optimization of Human iPSC Chondrogenesis with Single Cell Transcriptomics

Rosier Awards and Closing Remarks

2:00 PM **Randy Rosier, MD, PhD**

eSocial 2:15 - 3:00 PM

Medicine of the Highest Order

UR Medicine

ROCMSK Training Program

The Annual CMSR symposium is the center piece of the NIH/NIAMS funded T32 program entitled “Rochester Musculoskeletal (ROCMSK) Training Program” at the University of Rochester Medical Center. This program is designed to provide interdisciplinary didactic and research training in musculoskeletal science.

The overarching goal of ROCMSK Training Program is to develop future generations of interdisciplinary musculoskeletal scientists and leaders of innovations. The program is administered in The Center for Musculoskeletal Research (CMSR) at the University of Rochester and integrates 21 highly-collaborative faculty with primary appointments in 7 academic and clinical departments. The CMSR and associated training faculty represent a highly integrated group of Mentors that provide research training opportunities in Bone Biology and Disease, Cartilage Mechanobiology, Arthritis, and Regenerative Therapies, Tendon Development, Repair and Regenerative Engineering, Muscle Biology and Disease, Drug Delivery, Fracture Repair and Bone Tissue Engineering, Musculoskeletal Infection, Stem Cells and Musculoskeletal Development and Regenerative Biology, and Skeletal Cancer Biology and Therapeutics, as can be seen from the abstracts featured in this symposium.

The education program ensures a comprehensive understanding of musculoskeletal science that is seamlessly accessible to all CMSR trainees at every academic level. ROCMSK training emphasizes basic and translational science education. The training experience aims to build competency in areas ranging from the most basic molecular and genetic studies to the design and execution of human clinical trials. This year, ROCMSK awarded 2 pre-doctoral and 2 post-doctoral training seats.

This symposium is a celebration of the Trainees’ accomplishments.

Pre-Doc T32 Trainees

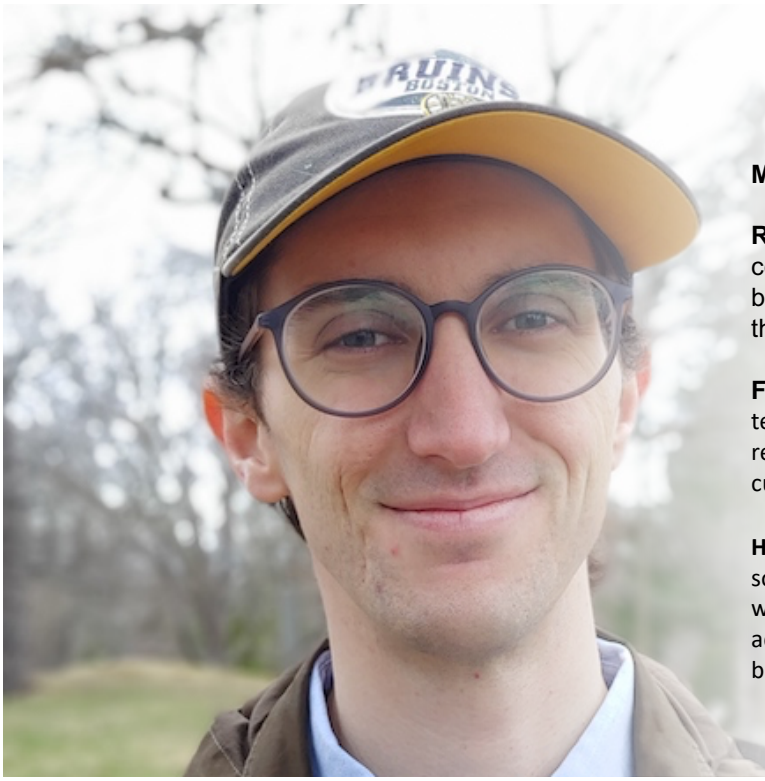

Nick James

BS, Boston University (2014)

Mentor: Jennifer Jonason, PhD

Research Interests: Development of a comprehensive understanding of chondrocyte biology and cartilage homeostasis as well as how they are altered and might be restored in disease.

Future Plans: Finishing up post-doctoral work and in ten years running own lab focused on developing regenerative medicines to treat (and someday cure) osteoarthritis.

Hobbies: Trying new restaurants, chilling out with (now socially distant) friends, and playing with his two cats while dreaming about the day he finally feels ready to adopt a dog. He also likes biking, hiking, and both board and video gaming

H. Mark Kenney

BA, University of Rochester (2017)

Mentor: Edward Schwarz, PhD

Research Interests: Studying the role of the lymphatic system in the development and progression of inflammatory arthritis.

Future Plans: As a future physician-scientist, his ideal career would consist of integrated clinical and research practices that continually inform each other.

Hobbies: Outside of science, he enjoys spending time with friends and family. Loves playing basketball and exploring the outdoors. Very passionate about binging TV shows and placing first in Mario Kart.

Post-Doc T32 Trainees

Anne Nichols, PhD

PhD, Virginia Tech (2018)

Mentor: Alayna Loiselle, PhD

Research Interests: Understanding the signaling pathways and mechanisms that govern cell- matrix interactions in mechanically active tissues, specifically tendon.

Future Plans: Start own lab focused on examining the cellular and molecular basis of tendon mechanobiology, in the context of how damage to the tendon matrix due to injury or overuse causes changes in the behavior of tendon cells in tendinopathy.

Hobbies: enjoy kayaking/hiking/camping with her husband and their two dogs. She also recently taught myself how to knit!

Alex Kotelsky, PhD

PhD, University of Rochester (2019)

Mentor: Whasil Lee, PhD

Research Interests: Multiscale biomechanics, focusing on applications to musculoskeletal diseases, to investigate the crosstalk between mechanics and biology.

Future Plans: In the next 5 years, plans on publishing multiple research articles and submitting Pathway to Independence (K99/R00) grant application. Ultimate goal is to have a career within academia and work as a successful researcher and professor.

Hobbies: Enjoys spending time with family cooking, playing board games, and playing with and taming their five pet hamsters. Loves spending time outdoors camping, hiking, kayaking, fishing, exploring state parks and traveling to different cities, amusement parks, and museums. Studies guitar and piano and enjoys learning new languages and cultures.

Spotlight Speakers

New Faculty Spotlight

Chike Cao, PhD

Assistant Professor - Department of Orthopaedics , Center for Musculoskeletal Research, University of Rochester Medical Center

Dr. Cao received an MS in Cell & Molecular Biology from the University of Arkansas, Fayetteville in 2004, and PhD in Pharmacology and Physiology from Rutgers New Jersey Medical School, Newark in 2007. After completing her post-doctoral tarining the Mayo Clinic and Duke University, Dr. Cao joined Weill Cornell Medicineas an instructor in 2017, before being recruited to the University of Rochester Medical Center and joining the CMSR as an Assistant Professor in the summer of 2020. Dr. Cao's research is focused on understanding the physiological roles of calcium channels in musculoskeletal development and regeneration, and the development of therapeutics to target these channels and/or their downstream factors to help prevent and treat musculoskeletal diseases. Her primary interest is to understand voltage-gated calcium channel signaling, and the molecular basis of the specific calcium-dependent cellular processes downstream of calcium channels, during bone and tendon formation and regeneration. More recently, she investigated the function of the L-type CaV1.2 Ca2+ channels—a channel previously considered to function only in excitable tissues—in non-excitable bones and tendons, and found that a gain-of-function mutant CaV1.2 promotes bone and tendon formation, including pathologies associated with these tissues such as hetertopic osssification, which is one of the foci of new lab in the CMSR.

Awards

2017 Harold M. Frost Young Investigator award
2017 Young Investigator Travel Grant, ASBMR, Denver, Colorado
2019 Blue Ribbon Poster Award, ORS 48th international Musculoskeletal Biology Workshop, Sun Valley, Idaho
2019 Alice L. Jee Young Investigator Award, ORS 48th international Musculoskeletal Biology Workshop Sun Valley, Idaho

New Faculty Spotlight
Chia-Lung Wu, PhD

Assistant Professor - Department of Orthopaedics , Center for Musculoskeletal Research, University of Rochester Medical Center

Dr. Wu received an MS in Materials Science and Engineering from the National Taiwan University in 2005, and PhD in Biomedical Engineering from Duke University in 2015. After completing his post-doctoral tarining at Washington University in Saint Louis, he joined the CMSR as an Assistant Professor in the Fall of 2020. Dr. Wu's research interest is to examine the role of genetic and epigenetic regulation in cell fate decisions into musculoskeletal lineages as well as onset and progression musculoskeletal diseases using multidisciplinary approaches including next-generation sequencing technology, bioinformatics, pluripotent stem cells, and animal models. Since his post-doctoral training, he has applied his expertise to study embryonic chondrogenesis using next-generation sequencing techniques (i.e., both bulk and single-cell RNA sequencing) as well as human induced pluripotent stem cells (hiPSCs) as a model system. He recently established a robust step-wise chondrogenic differentiation protocol for hiPSCs via specification of paraxial mesoderm. This protocol is built upon the elucidation of the gene regulatory network governing chondrogenesis and can efficiently generate clinically relevant, large scale numbers of chondrocytes without cell sorting. His new lab in the CMSR aspires to extend our understanding of the epigenetic regulation of chondrogenesis and limb development, and to provide novel insights into the homeostasis of cartilage, as well as the refinement of new strategies for cartilage repair and regeneration.

Awards
2014 The New Investigator Recognition Awards (NIRA), Orthopaedic Research Society (ORS)
2018 The New Investigator Recognition Awards (NIRA), Orthopaedic Research Society (ORS)
2019 NIH NIAMS K99/R00 Pathway to Independence Award – 1K99AR075899
2020 ON Foundation Award, Orthoregeneration Network Foundation

Guest of Honor

Randy Rosier, MD, PhD

Professor Emeritus of Orthopaedics and Rehabilitation and Biochemistry and Biophysics University of Rochester Medical Center

Dr. Rosier received an MS in biophysics from the University of Rochester in 1977, MD degree in 1978, and PhD in biophysics in 1979. After his Orthopaedic training at the University of Iowa, Dr. Rosier returned to Rochester to join the faculty of the Department of Orthopaedics and create an Orthopaedic Oncology service. In addition, Dr. Rosier established a molecular biology research program in the area of growth factor regulation of cartilage development and regeneration, and an Osteoporosis Center for the treatment of metabolic bone diseases.

In 2000, Dr. Rosier became Chairman of the Department of Orthopaedics, and established the Center for Musculoskeletal Research which he directed. The Orthopaedic research program of the Center, which focuses on bone and cartilage healing and regeneration, arthritis and gene therapy, tissue engineering, osteoporosis, and treatments for implant loosening and cancer bone metastasis, has become ranked as the number one NIH funded Orthopaedic research program in the United States. In March of 2007, Dr. Rosier discontinued his Departmental administrative roles to devote more time to directing a new Center of Translational Research, his ongoing research programs in osteoarthritis and skeletal lead toxicity, and his clinical practice of orthopaedic oncology.

Dr. Rosier served as a director of the American Board of Orthopaedic Surgeons, a member of the board of directors of the Orthopaedic Research Society and has been a member of the University of Rochester Medical Center Board, and the Advisory Council of the National Institute of Arthritis, Musculoskeletal and Skin Diseases. He has chaired the Education and Critical Issues Committees of the American Orthopaedic Association, and the Committee on Biological Implants of the American Academy of Orthopaedic Surgeons. He has authored over 140 peer reviewed publications, 30 book chapters, and 275 published abstracts on research topics, with a focus on molecular biology of skeletal tissues, osteoarthritis, osteoporosis, orthopaedic oncology, and clinician-scientist development.

Awards

2009 The Alfred R. Shands Jr, MD Award, American Ortho Association and the Orthopaedic Research Society
2009 Best Doctors in America for Tumor Surgery
1998 Dean's Professorship, University of Rochester
1995 Kappa Delta Award for outstanding orthopaedic research

Abstracts

Disclaimer

Title: **The periostin niche as a target for modulating myofibroblast differention to promote regenerative tendon healing.**

Presenting Author: Jessica E. Ackerman,

Co-Authors:

Lab PI / Mentor: Alayna E. Loiselle PhD

Abstract (3500 characters or 500 words Limit)

Tendon injuries are a major clinical problem, with poor patient outcomes due to tendon's fibrotic healing process. A main driver of fibrosis is thought to be persistence of matrix-producing myofibroblasts, and we have previously shown that α-SMA+ myofibroblasts are abundant at all stages of fibrotic tendon healing. While myofibroblasts are required for structural support and wound contraction following tissue injury, aberrant accumulation can initiate fibrosis via pathological matrix production. Periostin is a matricellular protein that has been linked to the progression of fibrosis in a number of other tissues, and is utilized in the heart to label matrix-producing myofibroblasts. We hypothesized that postn+ cells likewise represent activated myofibroblasts in the context of acute tendon injury, and aimed to better understand the relationship between periostin and a-SMA+ myofibroblasts to define therapeutic targets to attenuate fibrotic tendon healing.

To trace Postn-lin cells, Postn-MCM; Ai9 F/+ mice were used, in which tamoxifen treatment results in permanent TdTomato labeling of all cells expressing periostin. Both male and female 10-12-week-old mice underwent surgical transection and repair of the FDL tendon prior to tamoxifen treatment.

To determine the potential of Postn+ cells to differentiate into α-SMA+ myofibroblasts, Postn-MCM; Ai9 mice underwent surgical repair of the the FDL and were put on a diet of tamoxifen chow throughout healing until harvest at D28. Postn-lin cells are observed abundantly in both the bridging scar tissue and surrounding the injured tendon ends at D28. Interestingly, these cells appear to correspond with a thickened epitenon layer, suggesting that they are important for structural support during healing. We noted essentially no colocalization with α-SMA expression, disproving our hypothesis that these cells become α-SMA+ myofibroblasts in the context of tendon injury. Instead, they may provide an important supportive function, possibly through secretion of periostin into the scar tissue matrix.

To better understand the role of secreted periostin following tendon injury, we conducted co-immunofluorescence for both secreted protein and α-SMA in C57BL6/J mice from D3 to D28 after surgical repair. Interestingly, at D7 and 14, α-SMA+ myofibroblasts are found within a dense network of secreted periostin, suggesting that it may act as a niche for myofibroblast differentiation and/or function. Secreted periostin has been shown to be required for fibroblast-myofibroblast differentiation in models of lung and liver fibrosis, which may also be the case in the context of fibrotic tendon healing.

Collectively, these data suggest that both Postn+ cells and the secreted protein have distinct supporting roles during fibrotic healing. Knockdown of either periostin expression, or depletion of Postn+ cells themselves, has been demonstrated to attenuate fibrotic healing in a number of tissues. Here we have determined that periostin also plays a part in tendon healing, possibly as a matrix for myofibroblast differentiation. Targeting this novel periostin myofibroblast niche to modulate myofibroblast function/differentiation may therefore be a novel therapeutic strategy to reduce scarring during tendon healing.

Title: **Tissue-on-Chip (ToC) platform for modeling inflammation and fibrosis in tendon healing**

Presenting Author: Raquel Ajalik

Co-Authors: Victor Zhang, Rahul Alenchery

Lab PI / Mentor: Dr. Hani Awad & Dr. James McGrath

Abstract (3500 characters or 500 words Limit)

The etiology and basic mechanobiology of fibrosis in tendon are not completely understood, which has abated advancements in tendon therapies for decades. The difficulty in studying commonly multifaceted chronic and/or acute tendon injuries is their healing response, which involves intricate phases where a fibrovascular scar forms and never restores the gross, histological, or mechanical characteristics of native tendon. The lack of advanced research strategies into tendon injuries has prevented the development of targeted biological therapies. Current studies on tendon healing often rely on in vivo animal experiments, yet innovative in vitro human microphysiological systems (hMPS) or tissue-on-chip platforms, are emerging as versatile platforms that can incorporate human cells to better understand the biological basis of diseases and to de-risk and accelerate the translation of new therapies. This project aims to design and fabricate a tissue-on-chip platform to elucidate the pathobiology of tendon injury and aid the investigation of inflammatory mediators in tendon healing, particularly the interactions between tendon fibroblasts, vascular cells, neutrophils and monocytes, including macrophages during the acute inflammatory phase.

The tissue-on-chip was fabricated by integrating a silicon nitride ultrathin microporous membrane into a silicone based microfluidic device. The microporous membrane was sandwiched between layers, creating a defined basal channel and apical chamber for the co-culture platform. Polydimethylsiloxane (PDMS) was used as a pipette access layer into the basal channel, holding a vascular layer, and to create a media well for the top chamber housing a fibroblast-laden collagen gel. Anchoring support for the collagen tissue allows for directed fibroblast alignment. Murine primary tendon fibroblasts were suspended in type I rat tail collagen and cast into an adapted device consisting of the tendon holding layer and top chamber with anchoring rods to isolate the effects of a 10 ng/mL TGF-β1 treatment to the fibroblasts. Human fibronectin was introduced into the basal channel to facilitate HUVEC adhesion.

The initial design of the ToC platform enables viable cell seeding, appropriate hydrogel anchoring, live imaging, and IHC staining in a single device. Preliminary results in the fibroblast laden collagen hydrogel exhibited increased expression of α-Smooth Muscle Actin (α-SMA) upon TGF-β1 treatment compared to control ($n=5$, $p<0.001$), indicating elevated myofibroblast activation. We also demonstrated the feasibility of creating a vascular monolayer in the basal side of the porous membrane using HUVECs, which was verified by IHC staining of actin and VE-cadherin.

This platform enables a co-culture of tenocytes with endothelial cells in vitro to model the early stages of fibrosis through the induction of TGF- β1. We demonstrate the viability of a HUVEC monolayer in the basal side of our porous membrane as a first step to providing a vascular barrier to this co-culture device. The differentiation of fibroblast into the active myofibroblast phenotype through the increased expression of α-SMA indicates the feasibility of modeling for fibrosis to better understand the pathology and screen therapeutics. Ongoing experiments will investigate gene expression and secreted cytokines as well as the barrier integrity of the vascular layer upon dose-dependent TGF-β1 treatments, with plans to flow immune cells in the next phase.

Title: **TGF-β1 Activates mTORC1 Signaling in Mouse Flexor Tendon Fibroblasts**

Presenting Author: Rahul Alenchery

Co-Authors: Sylvia Zhong, Firaol Midekssa, Raquel Ajalik, Hani Awad

Lab PI / Mentor: Hani Awad

Abstract (3500 characters or 500 words Limit)

The incomplete understanding of the complex cellular and molecular processes involved in fibrotic tendon healing has hindered the development of biological therapies for true regenerative repair. TGF-β1 has been established as the main driver of fibrosis in renal, cardiac, lung, skin and tendon disease models through downstream α-smooth muscle actin (α-SMA) positive myofibroblast activation, excessive ECM production and inhibition of ECM degradation. Recently, the PI3K/AKT/mTOR pathway, the key regulator of a broad range of fundamental cellular processes, has also been implicated to play a central role in the progression of pulmonary, cardiac, renal and tendon fibrogenesis. However, while it has recently been implicated in tendon development, the molecular and mechanobiological mechanisms of the PI3K/AKT/mTOR pathway as a potential driver of tendon fibrosis after injury have yet to be investigated. Towards testing the central hypothesis that TGF-β1 regulates PI3K/AKT/mTOR signaling in mouse flexor tendon cells leading to the fibrotic tendon response to injury, we evaluated the effects of TGF-β1 treatment of tenocytes on PI3K/AKT/mTOR signaling and the associated activation of the myofibroblast phenotype.

To test this hypothesis, flexor tendons were excised from healthy C57BL/6 wildtype (WT) mice and processed for enzymatic tenocyte isolation. Isolated flexor tendon cells were treated with α-MEM media supplemented with ± 10 ng/mL TGF-β1 and analyzed at timepoints between 1-48 hours to account for the temporal kinetics of signaling responses to TGF-β1. qRT-PCR analysis was completed for genes Pik3ca, Pten, 4e-bp1 and Akt (n=3-4). Western blot analysis of target proteins included total and phosphorylated forms for PTEN, Akt, 4E-BP1, p70S6K, TSC2 and the loading control, β-actin (n=3-4). Separate samples were processed for immunostaining with α-SMA for confocal analysis.

As we hypothesized, we observe TGF-β1 to be critical in activating PI3K/Akt and downstream mTORC1/4EBP1 in WT mouse tenocytes. Through this TGF-β1 stimulation, we also observe fibroblasts to be significantly activated and undergo phenotypic transition into α-SMA positive myofibroblasts, the key effector cells in fibrotic states. From these findings, we propose that targeting the TGF-β1/mTOR axis in tendon healing states may provide novel therapeutic strategies. TGF-β1 signals through canonical Smad and non-canonical pathways, such as the PAI-1 coagulation cascade, to influence fibroproliferative behavior. The observed decreases in gene expression and phosphorylation of PTEN, a natural inhibitor of the PI3K/Akt/mTOR pathway, with TGF-β1 in turn implicates the involvement of complex feedback mechanisms in regulating PI3K/Akt/mTOR signaling. Our previous in-vivo studies observed the genetic deletion of PAI-1 to be mechanistically linked to PI3K/Akt/mTOR through PTEN. These observations further support an axis of TGF-β1/PAI-1/mTOR signaling in progressing fibrosis, which we plan to investigate in future studies.
Our results suggest that TGF-β1 mediates mTOR signaling to potentially regulate mechanisms associated with tendon fibrosis. Given the currently active clinical trials investigating the safety, tolerability and pharmacokinetics (NCT03502902) and the efficacy (NCT01462006) of mTOR inhibitors as disease modifying drugs for pulmonary fibrosis, the identification of mTOR as a mediator of fibrosis in tendon injury could lead to disease-modifying druggable targets.

Title: **Selective Inhibitors of Nuclear Export Differentially Impact Blood versus Bone Marrow-Derived Plasma Cells in Systemic Lupus Erythematosus**

Presenting Author: Jennifer L. Barnas

Co-Authors: Neha Nandedkar-Kulkarni, Nida Meednu, Jennifer Albrecht, Jennifer L. Barnas, Douglas G. Widman, Jennifer H. Anolik

Lab PI / Mentor: Jennifer H. Anolik

Abstract (3500 characters or 500 words Limit)

Background: Systemic lupus erythematous (SLE) is an autoimmune disorder with heterogeneous presentation and a multi-pronged pathogenesis. Although autoreactive plasma cells play a key role in SLE, they are still elusive targets. Selective inhibitors of nuclear export (SINE) were recently approved by the FDA for treatment of refractory multiple myeloma (selinexor). Our lab demonstrated that SINE abrogate lupus nephritis and significantly reduce autoreactive plasma cells in lupus prone NZBW/F1 mice. Here we investigated the impact of SINE on in vitro survival and antibody secretion of human plasma cells (PC) and how these classic PC functions are modulated by the bone marrow (BM) microenvironment.

Methods: Peripheral blood mononuclear cells (PBMCs) and bone marrow mononuclear cells (BMMCs) from healthy (n = 4) and SLE donors (n = 4), cultured in the presence of mesenchymal stromal cell secretome, were treated with KPT-335 for different periods of time. Number of antibody secreting cells (ASC) and PC survival were assessed by IgG ELISPOT and annexin V-propidium iodide flow based apoptosis assay, respectively. CD19+CD27hiCD38hi blood plasmablasts, CD19+CD27hiCD38hiCD138+ BM mature PCs and CD19-CD27hiCD38hiCD138+ BM long-lived PCs were sorted for transcriptomic analysis (controls: n = 7 and SLE: n = 9).

Results: Blood ASC were significantly reduced (IC50= 0.1uM) compared to BM ASC (IC50 = 10uM) after short-term ex vivo treatment with KPT-335 (24 hours). In long-term cultures (120 hours), there was a greater impact on BM PCs (IC50=0.1uM). We also examined the capacity of SINEs to induce apoptosis in different PC subsets. Blood plasmablasts from both healthy and SLE donors were reduced by 30-70% after SINE treatment for 48 hours. Of note, SINE treatment did not affect BM mature and long-lived PC. In transcriptomic analysis, BM PCs showed up-regulation of NFkB signaling and extra-cellular matrix receptor interactions (gene pathway analysis), and down-regulation of cell cycle signaling pathways when compared to blood PC. Mature and long-lived PC in lupus BM had a prominent interferon (IFN) gene expression signature compared to healthy controls. We are currently investigating the impact of type I IFN on PC survival and function.

Conclusions: SINEs represent a novel treatment approach for SLE. These results support the hypothesis that the effect of SINEs on PC depends upon the dose and duration of treatment, and is modulated by BM microenvironmental signals that orchestrate PC survival.

Title: Temporally Controlled Release of Periosteal Paracrine Factor Mimetics for Efficient Bone Allograft Healing: A Cell and Growth Factor Free Approach

Presenting Author: Sayantani Basu

Co-Authors: Amy Van Hove, Yiming Li

Lab PI / Mentor: Danielle Benoit

Abstract: (3500 characters or 500 words Limit)

Bone graft surgeries are the second most frequently performed tissue transplantation surgeries after blood transfusion. Despite being the gold standard for bone grafting, widespread application of autografts is hindered by complications from tissue-harvesting procedure and limited tissue volumes for transplantation. Therefore, bone allografts are used in situations where large tissue volumes are required for transplantation. Compared to autografts, allografts are associated with an increased risk of failure due to poor integration with host tissue, resulting in 60% failure rate at 10 years post-implantation. Healing deficiencies observed in allografts are due to absence of periosteum, the thin layer of vascularized and innervated tissue that surrounds all bone tissue, and coordinates bone healing in autografts. This thin layer acts as a reservoir of multiple cell types including stem cells and osteoprogenitors. However, these cells contribute only minimally to new tissue formation but instead orchestrate healing via paracrine signaling cascades. Therefore, we are exploiting our matrix metalloproteinase (MMP) degradable poly(ethylene glycol) (PEG)-based drug delivery depots as an acellular tissue engineered periosteum (TEP) to emulate paracrine factor temporal cascades observed during periosteum mediated autograft healing.

To do so, analysis of RNA sequencing data during bone regeneration was first performed to identify upregulated gene ontology pathways (Data obtained from [1]). The analysis showed 15 overlapping pathways were upregulated over the first 2 weeks of healing. 9 out of these 15 pathways were related to blood vessel morphogenesis and vascularization and levels of nerve growth factor (NGF) were significantly upregulated over the first 1-3 days. These data reveal the importance of temporal availability of neurovascular paracrine factors over the timecourse of bone healing. To recapitulate the temporal release of paracrine factors, peptides were selected as opposed to growth factors since peptides offer versatile synthesis methods, conjugation strategies, and higher stability *in vivo.* Paracrine peptide mimetics are tethered to the PEG chains *via* MMP degradable tethers with tunable degradation rates. To elucidate the kinetics of release to match paracrine factor availability, a model peptide is tethered *via* several MMP degradable linkers. For instance, model peptides tethered via IPVS ↓ LRSG-CG, displayed a pseudo first order release kinetics with rate constant of 3.65×10^{-3} h^{-1}.

Current studies are focused on further investigation of MMP degradable tethers and kinetics to match RNA sequencing data. We aim to achieve a burst release of NGF mimetic peptide within 1-3 days followed by a comparatively sustained release of vascular endothelial growth factor (VEGF) mimetic peptide Qk over longer time spans. This cell and growth factor free strategy will mimic the periosteal microenvironment to reduce graft failure rates and improve existing allograft transplantation therapies for bone defect repair.

Reference:

[1] Coates et al., Bone 127 (2019) 577–591

Title: **Emerging Methods for 3-Dimensional Volume Interrogation of Staphylococcus aureus Pathogenesis in the Osteocyte Canalicular Network**

Presenting Author: Karen de Mesy Bentley

Co-Authors: Chad Galloway, Gowri Muthukrishnan, Scott Echternacht, Elysia Masters, Stephan Zeiter, Jonathan Leckenby, Edward Schwarz

Lab PI / Mentor: Edward Schwarz

Abstract (3500 characters or 500 words Limit)

Introduction:
Our understanding of orthopaedic infections come from advances in transmission electron microscopy (TEM) imaging of murine models documented Staphylococcus aureus deformation, invasion and colonization of osteocyte canalicular networks of live cortical bone in establishment of chronic osteomyelitis. Our previous studies were limited by the 2-dimensional analysis of the bacterial occupation of the 3-dimensional (3-D) osteocyte canalicular network. One micron sectioning of epoxy embedded bone tissue is extremely labor intensive to locate a "needle in a haystack" presence of bacteria within canaliculi, we therefore interrogated paraffin embedded mouse bone and used a histochemical stain to identify the bacterial region of interest (ROI). We excised the ROI from the paraffin block and re-embedded into epoxy resin for serial sectioning with the Automated-Tape-UltraMicrotome (ATUMtome) to produce a 3-D volume rendering of the ROI.

Methods:
An archived paraffin block from a previous study of a 14 day S. aureus infected and decalcified mouse tibia, was sectioned at 5 µm and stained using Brown and Brenn (B&B) gram stain to identify a region of interest (ROI) of S. aureus biofilm within the osteocyte canalicular network. The ROI area was excised from the paraffin block, deparaffinized to water, post-fixed in 2.5% glutaraldehyde for 24 hours, then 1.0% osmium tetroxide for one hour, dehydrated in an ethanol series, and embedded block face down, into EPON/Araldite epoxy resin The resulting epoxy block was serially sectioned using a Boeckeler ATUMtome, which generated 264 sections that were mounted sequentially onto 4 inch wafers, stained with uranyl acetate and lead citrate then carbon coated. A ZEISS Gemini SEM collected serial digital images using backscatter mode (BSE). The digital images were aligned and Z-stacked utilizing ImageJ and Linear Stack Alignment with SIFT, manually segmented, using VAST Lite software, to produce a 3-D rendering of the ROI with infected osteocyte canaliculi.

Discussion:
Generally, locating a "needle in a haystack" presence of bacterial biofilm in bone tissue is technically challenging with standard TEM epoxy embedded bone tissue. Our new paraffin block method greatly reduced interrogation time. Importantly, the architectural integrity of both osteocyte lacunae and canaliculi of our re-embedded bone tissue was preserved allowing for identification of bacteria. The image quality collected using an SEM in BSE mode, was comparable to standard TEM imaging. The resulting 3-D rendering, surprisingly, revealed infected canaliculi, adjacent to, non-infected canaliculi, and lead us to hypothesize that osteocytes may be able to initially respond and resist infection in this 14 day infection model only to succumb in long term chronic infection. The 3-D image results revealing adjacent infected (70%) and non-infected (30%) canaliculi may explain reactivation of childhood S. aureus osteomyelitis up to 80 years later. Thus, 3-D volume imaging may help answer the question; Why is S. aureus infection of bone often incurable?

Title: **Sexual Dimorphism in TNF-Induced Inflammatory Erosive Arthritis**

Presenting Author: Kiana Chen

Co-Authors: Richard D. Bell, Edward M. Schwarz

Lab PI / Mentor: Homaira Rahimi

Abstract (3500 characters or 500 words Limit)

Background: Rheumatoid arthritis (RA) is characterized by chronic joint inflammation and is female predominant. The TNF-transgenic (TNF-Tg) mouse model of RA develops inflammatory arthritis and lung disease. Previously, we showed selective sexual dimorphism in the lung disease of these mice, as females die significantly earlier than males (1). Examination of joint disease showed differences in disease progression between same age sexes. However, whether this discrepancy is defined by a temporal versus more severe disease difference in females has not been determined. We hypothesized that females will have earlier and worse disease than males.

Methods: Synovial knee joint tissue from four 3 month old TNF females, five 5.5 month old TNF females (end stage), four 5.5 month old TNF males, and five 12 month old TNF males (end stage) were obtained and stained with H&E and TRAP staining. Histological scoring via a semi-quantitative method using degree of synovial inflammatory infiltrate, pannus invasion, and TRAP+ tissue, was utilized in randomized, blinded fashion. The composite of these ranking measures determined the total histology score.

Results: Using analysis of variance testing with Tukey's post-test, there was no significant difference in synovial inflammatory infiltrate, pannus invasion, TRAP score, or the total histology score between 5.5 month old and 12 month old TNF males. Notably, all groups reached the peak score possible for pannus invasion, including the 3 month old TNF females.

Conclusion: These preliminary results validate prior findings of females exhibiting earlier onset of disease than males, reaching peak synovitis between 3 and 5.5 months. Males, however, have a larger window of peak disease between 5.5 and 12 months. Furthermore, the disease severity in males, as measured by the synovial inflammatory infiltrate, does not reach peak scores, whereas the females do. This finding suggests there may be a sex-related factor limiting disease severity in males. We did note that the current scoring system appears to have a ceiling effect at the older ages, which will be minimized using computer software analysis in future studies.

References

1. Bell, R.D., Wu, E.K., Rudmann, C.A., Forney, M., Kaiser, C.R.W., Wood, R.W., Chakkalakal, J.V., Paris, N.D., Klose, A., Xiao, G.-Q., Rangel-Moreno, J., Garcia-Hernandez, M.L., Ritchlin, C.T., Schwarz, E.M. and Rahimi, H. (2019), Selective Sexual Dimorphisms in Musculoskeletal and Cardiopulmonary Pathologic Manifestations and Mortality Incidence in the Tumor Necrosis Factor–Transgenic Mouse Model of Rheumatoid Arthritis. Arthritis Rheumatol, 71: 1512-1523.

Title: **Biomechanical Comparison of Stemless Humeral Components in Total Shoulder Arthroplasty**

Presenting Author: Raymond E. Chen, MD

Co-Authors: Emma Knapp, Bowen Qiu, Anthony Miniaci, Hani Awad, Ilya Voloshin

Lab PI / Mentor: Ilya Voloshin/Hani Awad

Abstract (3500 characters or 500 words Limit)

INTRODUCTION: The purpose of this study was to compare initial fixation strength between various stemless and stemmed humeral components. A secondary objective was correlate component fixation strength of each implant with bone mineral density (BMD).

METHODS: Five different humeral stem designs were included in this study: three stemless (Sidus , Simpliciti, OVOMotion), one short stem (50 mm) and one standard stem (130 mm). 50 cadaveric human humeri were obtained. All samples underwent DXA scanning to determine BMD within the humeral head. The 25 samples with the lowest BMD were categorized as “Low”, while the 25 samples with the highest BMD were categorized as “High”, with the BMD threshold set at 0.35 g/cm2. Samples were then randomly divided into five equal groups and implanted with humeral components. Each group was then subdivided into low and high BMD subgroups. Each sample was then secured in custom fixtures on a biaxial biomechanical testing machine (Instron ElectroPuls 10000). Three differential variable reluctance transducers (DVRTs) (LORD MicroStrain) were fixed to the implants to detect micromotion in three planes. All samples underwent the same testing protocol, with axial loading followed by torsional loading. Axial loading consisted of cyclic loading for 100 cycles at 3 peak forces (220, 520 and 820 N). Torsional loading consisted of 100 cycles of internal/external rotation at 0.1 Hz at 6 peak torques, or until failure (± 2.5, 5, 7.5, 10, 12.5 and 15 Nm). Failure was defined as any bone fracture, implant detachment from anchor/stem or an excess of 50□ internal/external rotation. Micromotion was tracked throughout testing and the data from the three sensors were used to compute the total displacement value for each time point. Adjusted failure (AF) was calculated as defined by AF = torque of fully completed cycle + (% of complete failure cycle*2.5 Nm). Statistical analysis was performed to compare findings between groups and subgroups using one-way ANOVA.

RESULTS: OVOMotion implants demonstrated significantly less mean micromotion than Sidus and Simpliciti implants in low BMD samples during maximal axial loading (820 N), $p<0.05$. Standard stems failed at a significantly higher mean torque than all stemless designs, $p<0.05$. Within stemless designs, OVOMotion failed at significantly higher mean torque than Sidus, $p<0.01$. For low and high BMD samples, stemmed implants failed at a significantly higher mean torque than Sidus and Simpliciti, $p<0.05$. There was no significant difference between OVOMotion and Stemmed implants in low and high BMD samples during axial or torsional loading.

DISCUSSION: The findings from the study demonstrate that both implant design and bone mineral density play roles in the initial fixation strength of stemless humeral components. The OVOMotion implant, which is a central screw and peripheral cortical fit design, demonstrated greater fixation in low BMD samples when compared with Sidus and Simpliciti implants, which rely exclusively on metaphyseal fixation. The OVOMotion implant also behaved similarly to stemmed implants in both low and high BMD samples.

Title: **Next generation sequencing as a potential diagnostic tool for complex musculoskeletal infections.**

Presenting Author: Brandon Dexter, BS

Co-Authors: Yoonjung Choi, BA; Thomas Sajda, MD PhD; Christopher Beck, PhD; Irvin Oh, MD

Lab PI / Mentor: Irvin Oh, MD

Abstract (3500 characters or 500 words Limit)

Background: Accurate identification of dominant pathogens in musculoskeletal infections (MSKIs), including diabetic foot ulcers (DFUs), can have critical and lifesaving information for patients suffering from bacterial infections, potentially decreasing mortality and the economic burden on the US healthcare system. Standard culture has shown high false-positive and false-negative rates. Next generation sequencing (NGS) has the potential to serve as a more accurate and efficacious method in identification of the main pathogens in polymicrobial infections. NGS can detect and sequence entire genomes of all bacteria in a given specimen with the resistance genes to antibiotics, which allows clinicians to tailor a specific and effective treatment for each patient. We investigated the potential use of NGS for identification and quantification of microorganisms in infected DFUs. We hypothesize that NGS will aid identification of dominant pathogens and provide a more complete profile of microorganisms in infected DFUs compared to the standard culture method.
Methods: To determine the efficacy of this clinical application, 30 DFU infected patients, under the care of an orthopaedic foot and ankle subspecialist, were evaluated over the course of 1 year. All 30 patients underwent surgical intervention from which tissue samples were collected and evaluated using both NGS and standard culture.
Results: Pathogens were identified for 96% (29 of 30) of patients using both standard culture and NGS. Standard culture identified Staphylococcus aureus (58.6%) as the primary pathogen followed by coagulase-negative Staphylococcus (24.1%), Corynebacterium striatum (17.2%) and Enterococcus faecalis (17.2%). NGS identified Finegoldia magna (44.8%) as the primary pathogen followed by Staphylococcus aureus (41.4%) and Anaerococcus vaginalis (24.1%). The average number of pathogens identified by NGS ranged from 1-11 while standard culture ranged from 1-6 with an average value of 5.1 and 2.6 respectively.
Conclusion: This study demonstrates that, while standard culture has been utilized to identify organisms along with their respective pharmacologic resistances, NGS has the potential to provide a more complete profile of microbiomes within DFU infections. While more studies are needed to confirm these results, NGS as a diagnostic tool could improve the prognosis of countless patients, especially those who suffer from recurrent and persistent infections.

Title: **Analysis of the Anterior Drawer Test in ACL Injured Mouse Models**

Presenting Author: Srilatha Edara

Co-Authors: Alexander Kotelsky, Sandeep Mannava, Whasil Lee

Lab PI / Mentor: Whasil Lee / Alexander Kotelsky

Abstract (3500 characters or 500 words Limit)

Anterior cruciate ligament (ACL) injuries are common with an annual incidence of ~150,000 cases in US, and 50% of ACL-injury patients develop post-traumatic osteoarthritis (PT-OA) within 5-15 years post-injury. Sexual dimorphism has been observed: females have 2~4 times higher risk to tear the ACL and females have a higher prevalence of knee OA than males. Our lab has established a non-invasive mechanically-induced ACL-injury mouse model using a custom-built device to investigate the adaptive progression of PT-OA and sexual dimorphism of longitudinal cartilage degeneration. In this study, we tested our hypothesis that ACL injured female mice will exhibit a higher change of knee laxity compared to the ACL-injured male mice by means of X-Ray-based drawer test over 2 months post ACL-injury. Briefly, uninjured and ACL-injured female and male C57BL/6 mice at age of 8 weeks (n=6-10/group) were sacrificed at 0- and 8-weeks post injury. The mice were laterally placed in the X-ray machine (Faxitron) and taped to a custom-designed Styrofoam block. X-Ray images were obtained with and without the application of a 0.2 N weight used to pull the murine tibia anteriorly. The images were analyzed using a custom algorithm in MATLAB and we quantified the initial femoral position, final femoral position, and the displacement of the femur relative to the center of the tibial plateau. We confirmed the consistent position of knee joint angles at 91.1 ± 6.6°. A two-way ANOVA test was used to compare the groups across gender and time-points.

Our data of the initial femoral position, final femoral position, and displacement of the femur consistently showed an increase in the laxity of the murine joint in the injured mice relative to the uninjured mice for both 0 and 8 weeks post-ACL injury, except for the displacement in male mice at 8 weeks post injury. This increase indicates the onset of PT-OA and osteophyte formation which was shown in the X-ray images at 8-week post injury. Osteophytes may alter mouse gait pattern and may also prevent the displacement upon application of the 0.2 N force. Interestingly, we observed that while initial and final femoral positions in injured female mice at 8 weeks post-ACL injury was lower than in injured male mice (65% vs. 81%, 72% vs. 81%), the anterior displacement in female mice was elevated (7% vs. 3%). In summary, we observed that the laxity of the injured knee joint is greater than the uninjured knee joint. Additionally, we noticed a difference between injured male and injured female mice at 8 weeks post-ACL injury presumably due to the changes in gender-related differences in the growth and development of PTOA. It is also possible that there were gender-related differences in the development of osteophytes, which impacted the laxity of the knee joint. To quantify the osteophyte formation in the 8-week post-ACL injured mice, we plan to compare the osteophyte levels measured by micro computed tomography (μ-CT) in male and female mice.

Title: **Development of Peptide-Functionalized Hydrogels to Support Periodontal Ligament Cell Bioactivity**

Presenting Author: David Fraser

Co-Authors:

Lab PI / Mentor: Danielle Benoit

Abstract (3500 characters or 500 words Limit)

Introduction. Multipotent cells are present in the periodontal ligament (periodontal ligament cells – PDLCs) which differentiate and contribute to the formation of new bone and cementum in response to the appropriate extracellular matrix (ECM). While PDLCs can be isolated and cultured ex vivo, numerous hurdles remain for realizing PDLCs' regenerative potential. In particular, the appropriate scaffold cues for controlling PDLC activity are still unknown. ECM proteins within the PDL contain peptide motifs to which PDLCs bind via cell surface integrins. Poly(ethylene glycol) (PEG) hydrogels hold particular promise as a regenerative biomaterial by acting as a tunable synthetic matrix for precise presentation of ECM cues such as peptide motifs. Therefore, the purpose of the current study was to utilize peptide-functionalized PEG hydrogels as a synthetic PDL ECM to test the role of PDLC integrin-matrix binding in supporting PDLC bioactivity.
Methods. PDLCs were obtained from 3rd molars of 3 age-matched, healthy subjects, characterized, and encapsulated within PEG hydrogels. Hydrogels were formed via radical-mediated thiol-ene polymerization of 8-arm PEG-norbornene (-ene) with a matrix metalloproteinase (MMP)-degradable peptide crosslinker GKKCGPQGIWGQCKKG (cysteine residues (C) providing -thiol groups) and integrin alpha5beta1 and alphavbeta3-binding peptide ligand RGD (CGRGDS), integrin alpha2beta1-binding collagen-mimetic peptide ligand GFOGER (GCG(GPP)5GFOGER(GPP)5G), and/or a scrambled control peptide (CGRDGS). A design of experiments approach was used to identify the contributions of RGD and GFOGER binding to key metrics of PDLC cementogenic/osteogenic differentiation, alkaline phosphatase (ALP) activity and PEG matrix mineralization.
Results. All PDLCs exhibited mesenchymal cell surface marker and high (>90%) expression of integrins alpha2beta1 and alpha5beta1, while expression of integrin alphavbeta3 varied from 51 – 95% between cells from different subjects. PDLCs spread and maintained >90% viability within PEG hydrogels and showed a 5 to 8-fold increase in ALP activity compared to PDLCs cultured on tissue culture plastic. PDLC ALP activity and matrix mineralization showed a dose-dependent response to RGD and GFOGER ligands separately, and demonstrated a complex, additive response to both ligands in combination. ALP activity in general was maximized with high concentrations of RGD and in PDLCs from subjects with high expression of integrin alphavbeta3, while matrix mineralization was elevated when GFOGER was presented together with the RGD peptide.
Conclusions: This study demonstrates that peptide-functionalized PEG hydrogels are a versatile biomaterial that supports PDLC bioactivity. Integrin binding within this synthetic ECM plays a complex role in driving both PDLC differentiation, as peptide compositions which maximize ALP activity do not necessarily support matrix mineralization. Furthermore, subject-to-subject PDLC variability significantly affects biomaterial-related outcomes. Thus, future studies will aim to identify mechanisms underlying integrin-mediated PDLC bioactivity, and the matrix characteristics which best support the regenerative potential of PDLCs from a wide range of patients.

Title: **Ex vivo culture of mouse bone marrow-derived hematopoietic stem cells**

Presenting Author: Hiroki Kawano

Co-Authors: Yuko Kawano, Mark W. Lamere, Caitlin Gordnier, Charles O. Smith, and Roman Eliseev.

Lab PI / Mentor: Laura M. Calvi

Abstract (3500 characters or 500 words Limit)

Hematopoietic stem cells (HSCs) are self-renewing and orchestrate the homeostasis of blood systems by giving rise to multi-lineage blood cells. In the clinic, HSCs play an essential role in hematopoietic stem cell transplantation to cure various kinds of blood and immune diseases by restoring normal hematopoiesis. In mouse experiments, the functions of HSCs have been extensively been researched. However, ex vivo culture of HSCs remains challenging, with rapid loss of HSC self-renewal and multipotency. To develop the ex vivo culture of mouse HSCs, we have carefully adapted recently published previous methodology (Wilkinson et al). First, we performed bone marrow-derived mouse HSC culture, where HSCs are isolated with automated cell separator (autoMACS Pro Separator) and cell sorter. In this protocol, we separated lineage-negative cells (Lin-) from the bone marrow (BM) cells harvested from C57BL6j (CD45.2) wild type mice and subsequently sorted out HSCs defined as Lin-ckit+Sca-1+CD34-/low. We cultured HSCs in fibronectin-coated 96-well plates in the F12 complete medium supplemented with cytokines (100 ng/ml TPO and 10 ng/ml SCF) and polyvinyl alcohol as a replacement for serum albumin. Despite successful HSC isolation, we noticed that L-glutamine addition (2mM) is required for HSC expansion, since there was the culture failure in the glutamine non-enriched medium. According to the recent report by Wilkinson et al (Nature, 2019), we utilized c-kit positive separation and defined HSC phenotypically as Lin-CD34-c-kit+Sca-1+CD150 (SLAM) +cells. Critical advantages of this strategy are that c-kit positive separation can result in the shortening of sorting time per mouse (25min to 5 min, $p<0.05$), in addition to better identification of CD34-negative population compared to previous protocol. 2,000 to 4,000 cells per mouse were collected compared to 12,000 cells per mouse in the standard protocol, which suggests more strictly defined HSCs can be attained in the revised method. We have also succeeded in expanding HSCs ex vivo (30 fold increase in cell number with 62% of c-kit+Sca-1+ in Lin- and 50% CD150+ in KSL gate on day7), but experienced the difficulty to maintain HSC potential while preventing cell differentiation at later time points in the culture system. In summary, the ex vivo culture of HSCs requires the careful cell handling and it could be a breakthrough for establishing long-term expansion of HSCs. This in vitro HSC expansion could be instrumental in devising transplantation models that do not require conditioning of the bone marrow with radiation, and increasing the opportunities to modulate HSCs in vitro.

Title: **Treatment Patterns, Trends, and Patient Reported Outcomes for Lateral Epicondylitis**

Presenting Author: Alan Hwang, MD

Co-Authors: Raymond Chen, MD; Serena Liu, MD; Ilya Voloshin, MD; Michael Maloney, MD

Lab PI / Mentor: Michael Maloney, MD

Abstract (3500 characters or 500 words Limit)

Introduction
Lateral epicondylitis is the most common cause of elbow pain. Treatment for lateral epicondylitis is largely non-operative. Recent literature suggesting poorer long-term outcomes with corticosteroid injections has made treating lateral epicondylitis in this manner more controversial. PROMIS outcome data has been recently validated for lateral epicondylitis and orthopaedic elbow procedures. This retrospective chart review study examines patient characteristics, treatment patterns, and examines PROMIS scores in lateral epicondylitis.

Methods
A total of 402 elbows in 366 patients were identified in a retrospective chart review. Patients treated for lateral epicondylitis between January 1, 2015 and December 1, 2015, were included in this study. Demographic and treatment data were collected along with PROMIS scores. Statistical analysis was used to determine if there were any significant differences amongst treatment types as well as other patient factors including diabetes status, sex, age, and other co-morbidities.

Results
Lateral epicondylitis was managed by orthopaedic hand surgeons (n = 136, 33.8%), orthopaedic sports medicine surgeons (121, 30.1%), and primary care physicians (103, 25.6%). For those treated by orthopaedic surgeons, 43.9% were managed completely with non-invasive methods, 56.1% received corticosteroid injections, and 11.1% received surgery. For those receiving corticosteroid injections, 36.9% had multiple injections with a mean of 289 days between the first and second injection. 48.0% of all patients only sought treatment once and did not return for a second clinic visit.

PROMIS outcome scores at initial visit did not differ based on their eventual treatment, but females were found to have significantly higher PROMIS depression (52.5 vs 45.7, $p < 0.01$), pain interference (60.8 vs. 56.8, $p = 0.01$), and lower physical function (43.5 vs 48.6, $p < 0.01$) scores than men at their initial visit.

Discussion and Conclusion
Although lateral epicondylitis is a commonly treated disorder, there are few published data on actual treatment patterns of this condition in the United States. This study was able to quantify the treatments of lateral epicondylitis and found that among those treated by orthopaedic surgeons, greater than 50% of patients treated for lateral epicondylitis received corticosteroid injections. Corticosteroid injections have previously been associated with worse long-term outcomes in both surgical and non-surgical patients, so the fact that this practice is so commonplace is notable.

As most of the patients who do well after the treatment of lateral epicondylitis presumably do not return to clinic for a follow-up exam, bias is introduced in those who have multiple clinic visits and multiple PROMIS scores, as they are more likely to be the patients who have worse outcomes. 48.0% of all patients were only seen once for lateral epicondylitis, likely indicating that their clinical course improved to the point where they did not want to seek further treatment. Analysis of initial PROMIS scores suggests that women with lateral epicondylitis are more likely to have worse depression, pain, and lower physical function than men prior to seeking treatment with an orthopaedic surgeon. Follow up PROMIS data is limited in the study population, and future studies focusing on follow up scores would give more data about outcomes of different treatments in lateral epicondylitis.

Title: **DNA damage in chondrocytes may initiate osteoarthritis development**

Presenting Author: M. Nick James

Co-Authors: Sarah E. Catheline, Richard Bell, and Jennifer H. Jonason

Lab PI / Mentor: Jennifer H. Jonason, Danielle S.W. Benoit

Abstract (3500 characters or 500 words Limit)

Osteoarthritis (OA), the most common and most expensive form of arthritis, is characterized by progressive loss of articular cartilage, however, the exact molecular mechanisms responsible for OA onset are still unclear. Aging is known to be among the most important risk factors associated with OA development. However, while aging is thought to be a consequence of accumulated DNA damage, the relationship between DNA damage and OA is not clear. Our laboratory has found that aged articular chondrocytes have increased inflammatory NF-κB activation and that enhanced IKKβ/NF-κB activation in chondrocytes accelerates spontaneous OA development in relatively young mice. DNA double-strand breaks (DSBs), a particularly toxic form of DNA damage, are also known to activate IKKβ which, in turn, promotes inflammatory NF-κB signaling. Thus, we hypothesize that accumulation of DNA damage in aging leads to chronic proinflammatory signaling that ultimately results in degeneration of articular cartilage and OA onset. To investigate the inflammatory role of DNA damage in OA development, we treated ATDC5 chondroprogenitors with the topoisomerase inhibitor etoposide which induces DNA DSBs. We demonstrated that etoposide effectively produces accumulation of DNA DSBs in ATDC5 chondroprogenitors and increases NF-κB activation by western blot. Etoposide treatment also increased in vitro expression of NF-κB and IRF gene targets including proinflammatory cytokines, catabolic matrix enzymes, and interferon-stimulated genes. We are currently in the process of developing a genetic mouse model which allows inducible, cartilage-specific induction of DNA DSBs through the intron-encoded endonuclease IPpoI. As proof of concept, we transfected ATDC5 cells with an expression vector encoding NLS-I-PpoI which resulted in increased proinflammatory and hypertrophic chondrocyte gene expression. These results suggest that DNA damage-induced inflammation may play a role in OA development. In the future, we plan to use cartilage-specific, IPpoI-induced DNA damage to study the effects of DNA damage on OA development. Understanding the impact of DNA DSBs on OA pathogenesis could inform development of novel OA therapeutic strategies that interrupt signaling pathways which mediate inflammation in OA.

Title: **Defining the Differential Function of Tendon Intrinsic and Extrinic S100a4+ Cells during Tendon Healing**

Presenting Author: Kendra W. Jones

Co-Authors: Jessica E. Ackerman, Alayna E. Loiselle

Lab PI / Mentor: Alayna E. Loiselle

Abstract (3500 characters or 500 words Limit)

Tendon healing is limited due to a scar mediated healing process that causes excess scar tissue formation and subsequent decrements in mechanical properties and range of motion (ROM). Successful tendon tissue engineering to replace or repair injured tendon has been limited largely due to an incomplete understanding of the cell populations involved in the scar mediated tendon healing process. We have previously shown that S100a4 is expressed by nearly 70% of the cells in the adult tendon. We have also demonstrated that global depletion of S100a4+ cells using S100a4-TK mice causes decreased mechanical properties and impaired ROM. Collectively these data suggest a central role for S100a4+ cells in tendon healing, and therefore generation of successful tissue engineering constructs. However, there is clear evidence that S100a4+ cells are a combination of tendon-derived and non-tendon derived cells. Cell origin has a substantial impact on cellular fate and function, as such delineating the functions of tendon-derived and non-tendon derived cells is critical to understanding the healing process. Mechanistically, S100a4+ cells contribute to an α-SMA+ myofibroblast fate. Myofibroblasts are critical for proper wound healing but can drive pathological fibrosis when dysregulated and lead to further impairments in tendon ROM and mechanics. It is critical to understand if the S100a4+ cell contribution to myofibroblast fate is origin dependent. Using a murine model of tendon allografting we have defined the tendon-specific S100a4+ cell contribution to healing and myofibroblast fate.

At 10-12 weeks of age male and female mice underwent tendon allograft surgery. The allograft is performed by isolating a section of the flexor digitorum longus (FDL) tendon from the hind paw of a 'donor' mouse and implanting the tendon graft into an equally sized defect in the tendon of the 'recipient' mouse. C57Bl/6J mice were used as recipients in all experiments. Donor tendons were harvested from either S100a4Cre;Rosa- Ai9 mice, labeling S100a4-lineage cells and their progeny with TdTomato (Red) or S100a4-GFPpromoter++ mice, which express GFP under control of the S100a4 promoter (S100a4active) and indicate active expression of S100a4. S100a4lineage tendon recipient (RFP) and S100a4active recipient mice (GFP) were harvested at D14 for histological and immunofluorescent analyses. Myofibroblasts were identified with an anti-αSMA-FITC antibody. Expansion of S100a4Lineage cells from the tendon graft were observed in the bridging tissue between the tendon graft and donor tendon confirming the contribution of tendon-derived S100a4+ cells to the healing process. Tendon graft-derived S100a4active cells were also observed in the bridging scar tissue, indicating the maintenance of S100a4+ expression following tendon grafting. We show that a subset of S100a4active cells differentiate into α-SMA+ myofibroblasts during tendon graft healing. However, many S100a4+ active cells did not go on to a myofibroblast fate by day 14 post-surgery. To define the function of tendon-derived S100a4+ cells, we are currently using the allograft surgery model with S100a4-TK donor tendons for inducible depletion of tendon-derived intrinsic S100a4+ cells.

This study will help define the differential functions of tendon-derived and non-tendon-derived S100a4+ cells during tendon healing, which will inform the ideal cellular composition of successful tendon tissue engineered construct.

Title: **Radiotherapy induces skeletal muscle physiologic deficits in a mouse model of pediatric rhabdomyosarcoma**

Presenting Author: Jacob Kallenbach

Co-Authors: Nicole Paris, John Bachman, Romeo Blanc, Carl Johnston, Eric Hernady, Jacqueline Williams, Joe Chakkalakal

Lab PI / Mentor: Dr. Joe Chakkalakal

Abstract (3500 characters or 500 words Limit)

Rhabdomyosarcoma (RMS) is the most common pediatric soft tissue sarcoma, accounts for 5% of all childhood cancers, and has a 5-year pediatric cancer survival rate of ~80%. RMS consists of aggressive, malignant, undifferentiated, and myogenic cells, whose treatment involves a combination of surgery, chemotherapy, and ionizing radiation therapy (radiotherapy). Even though childhood cancer survivors are living well into adulthood, they suffer from the repercussions of cytotoxic cancer therapies. 70% of pediatric sarcoma surviors treated with radiotherapy display skeletal muscle atrophy, excessive extracellular matrix accumulation (fibrosis), lower lean muscle mass, muscle weakness, muscle fatigue, and chronic inflammation from the irradiated tissue sites. As the primary force generators responsible for musculoskeletal movement, skeletal muscle functional deficits are intricately connected to deficits in quality of life for childhood cancer survivors. The key progress made in the field, forming the foundation of this presentation, is our development of a murine model for radiation-induced skeletal muscle decline relevant to treat rhabdomyosarcoma (RMS) tumors, in which there are 350 new cases of RMS in the United States yearly. Utilizing the innovative small animal research radiation platform (SARRP), we investigated the effects of targeted radiation on a localized RMS tumor implanted into a 4-week old mouse calf muscle. The experimental methods used to generate our data as well as interrogate these murine phenotypes are next-generation sequencing (NGS), quantitative reverse-transcriptase polymerase chain reaction (qRT-PCR), conventional immunofluorescent microscopy, second harmonic generation (SHG) imaging, and our ex vivo muscle contraction system. We hypothesized that targeted irradiation of RMS tumor-bearing pediatric mice at clinically relevant doses will approximate the physiologic deficits experienced in adult survivors of childhood cancer. Our fractionated irradiation approach successfully eliminates >95% of implanted RMS tumors in mice. At 4 weeks after the first fractionated radiation dose (4wpi), our data demonstrate significant muscle fiber atrophy, decreased myonuclear number, decreased muscle stem cell number, attenuated skeletal muscle force generation capacity, excessive extracellular matrix deposition, upregulated fibrotic gene expresion signaling, and persistent expression of inflammatory-related C-C chemokine receptor type 2 (Ccr2) signaling from the irradiated muscles. These physiologic, functional deficits present in irradiated fast-contracting extensor digitorum longus (EDL) muscles and irradiated slow-contracting soleus (SOL) muscles are exacerbated in RMS tumor-bearing mice. Next, we sought to determine if inhibiting inflammatory-mediated Ccr2 signaling will improve the functional deficits present in irradiated EDL and SOL muscles. We found that systemic CCR2 inhibition (CCR2i) did not significantly improve muscle function at 4wpi. Future studies will exploit our RMS mouse model to elucidate other therapeutic approaches to mitigate both the early and late effects of pediatric radiotherapy on skeletal muscle tissues with the clinical goal to augment the functional quality of life of childhood cancer survivors.

Title: **Investigating Murine Joint-Draining Lymphatics: Lineage Tracing and Single Cell RNA Sequencing Reveal Evidence that Popliteal Lymphatic Muscle Cells and their Progenitors Represent Distinct Cell Types Divergent from Skeletal and Vascular Muscle Cells**

Presenting Author: H. Mark Kenney

Co-Authors: H. Mark Kenney, Richard D. Bell, Elysia A. Masters, Lianping Xing, Christopher T. Ritchlin, Edward M. Schwarz

Lab PI / Mentor: Edward M. Schwarz

Abstract (3500 characters or 500 words Limit)

Previous studies demonstrated that tumor necrosis factor transgenic (TNF-Tg) mice with inflammatory arthritis have damaged lymphatic muscle cells (LMCs) and eventual loss of popliteal lymphatic vessel (PLV) contractions associated with severe joint disease by in vivo imaging (1). Ex-vivo assessment of TNF-Tg PLVs formally demonstrated a progressive reduction in PLV contractility isolated from the damage to the afferent joint and efferent lymph node (2). Remarkably, anti-TNF therapy in flaring TNF-Tg mice recovers these PLV-LMCs and PLV contractions concomitant with amelioration of arthritis (1). As this regenerative process is critical for resumption of joint function, knowledge regarding PLV-LMC progenitor origins and physiology is needed. Surprisingly, LMCs express an enigmatic actin profile with co-existing striated and smooth muscle actin isoforms (3), which is incompatible with the differentiation of known muscle progenitors. To determine PLV-LMC origin, we tested the hypothesis that PLV-LMCs are derived from previously characterized skeletal or vascular smooth muscle cell (VSMC) progenitors via lineage tracing studies in mice. We also utilized these lineage tracing models to specifically isolate PLV-LMCs and VSMCs for comparative single cell RNA sequencing (scRNAseq) transcriptomic analysis.

Constitutive Cre and tamoxifen-inducible CreER models were crossed into Ai9-tdTomato reporter lines for lineage tracing of PLV-LMCs during neonatal development. Induction of the CreER was achieved with 0.1 mg/g of tamoxifen administered intraperitoneal on postnatal days 10 – 13 (P10 – 13). All cohorts were sacrificed at both P21 and/or after 6-weeks. Pax7-Cre and MyoD-iCre animals were used to study skeletal muscle cell origin, while Prrx1-Cre/CreER and NG2-Cre/CreER mice were used to trace VSMC progenitors by tdTomato (tdT) expression visualized by ex vivo whole mount immunofluorescent microscopy of PLVs. The NG2-Cre;tdT model was also utilized for fluorescence activated cell sorting (FACS) of tdT+ PLV-LMCs and VSMCs with downstream scRNAseq analysis on a 10X genomics platform.

We demonstrate that PLV-LMCs originate from Pax7-/MyoD-/Prrx1+/NG2+ progenitors prior to P10, and from previously unknown Pax7-/MyoD-/Prrx1+/NG2- progenitors during development after P10. In addition, our preliminary scRNAseq results suggest that mature PLV-LMCs are transcriptionally distinct muscle cells.

This is the first study to describe the unique origin of PLV-LMC progenitors and to assess the distinct characterization of mature PLV-LMCs using a scRNAseq approach. Our analysis suggests that PLV-LMCs do not derive from skeletal muscle progenitors with Pax7- and MyoD-negativity. In addition, PLV-LMCs appear to originate from similar Prrx1+/NG2+ progenitors to VSMCs, but subsequently derive from distinct Prrx1+/NG2- progenitors prior to P10 to become transcriptionally unique muscle cells. Thus, future work elucidating the PLV-LMC lineage, and defining specific markers of PLV-LMCs, will catalyze the development of LMC targeted therapies for diseases with lymphatic involvement, such as inflammatory arthritis.

Acronyms: Pax7 = Paired Box Protein 7; MyoD = Myogenic Differentiation Protein 1; Prrx1 = Paired Related Homeobox 1; Neural Glial Antigen 2 = NG2

1. Bouta et al. 2018. Nature Reviews Rheumatology. 14(2):94-106.
2. Scallan et al. 2020. BioRxiv. doi: https://doi.org/10.1101/2020.09.22.309070 3. Muthuchamy et al. 2003. The FASEB Journal. 17(8):920-922.

Title: **Targeted Inducible Depletion of Scleraxis-lineage Cells During the Proliferative Healing Phase Significantly Impairs Flexor Tendon Mechanical Integrity**

Presenting Author: Antonion Korcari

Co-Authors: Katherine Best

Lab PI / Mentor: Alayna Loiselle

Abstract (3500 characters or 500 words Limit)

During healing, tendons produce a fibrotic tissue by deposition of abundant and disorganized ECM. The persistent fibrotic tissue results in permanent impairment of function and significantly increases the risk of re-injury. No therapies that promote regenerative tendon healing exist, and this is mainly attributed to lack of comprehensive understanding of the cellular and molecular events that take place during tendon healing. Scleraxis (Scx) is the earliest detectable marker for differentiated tendon cells. During adult tendon healing, Scx expression is required for complete wound healing. Recently, we inducibly depleted ScxLin cells prior to injury and we found that depletion of ScxLin cells resulted in tendons with increased biomechanical properties However, there is a knowledge gap on the functions of ScxLin cells in contrast to Scx as a transcription factor. In this study, we hypothesized that depletion of ScxLin cells during the proliferative phase (D14-18 post-repair) results in FTs with impaired ScxLin-based cell bridge and impaired biomechanical properties since at this phase, ScxLin cells are associated with matrix deposition and are significant contributors to the myofibroblast fate. To simultaneously deplete ScxLin cells and visualize the non-depleted ScxLinAi9 cells we generated Scx-Cre+; Ai9F/+; DTRF/+mice. To deplete ScxLin cells, 20ng of diphtheria toxin (DT) was injected into the hindpaw for 5 consecutive days. Scx-Cre+; Ai9F/+; DTR+/+ mice were also injected with DT and served as controls. 10-12 week old mice underwent complete transection and repair of the FTs in the right hindpaw. Between the 14th and the 18th day post-repair, DT was injected in the hindpaw to deplete ScxLin cells during the proliferative phase. Hindpaws were harvested at 28 days post-repair. Endogenous fluorescence (EF) of the ScxLinAi9 cells, from cryosectioned samples was detected using a fluorescent microscope. Uniaxial displacement-controlled stretching of 0.1% strain per second until failure was applied. Depletion of ScxLin cells during the proliferative healing phase (D14-18) results in the production of a thinner ScxLin-based cellular bridge and significantly impairs both structural (CSA, peak load, stiffness) and material properties (peak stress, modulus) of the healing FTs. In this study, we showed that depletion of ScxLin cells during the proliferative phase of healing results in production of a thinner ScxLin-based cell bridge and significantly impairs the structural and the material integrity of the FTs at 28 days post-repair. Based on our data, at this phase, ScxLin cells are required for a successful healing since they are associated with matrix deposition and are a significant contributor to myofibroblasts which actively deposit matrix and assist with the wound healing. Strikingly, these data are in contrast to our previous work in which ScxLin cells were depleted prior to injury.Collectively, these data suggest temporally-distinct functions of ScxLin cells during tendon healing. This is the first study to inducibly deplete ScxLin cells during tendon healing and delineate their roles in the proliferative phase. Understanding the roles of the ScxLin cells during healing will open new avenues in the tendon field by highlighting the importance of targeting specific cell populations and at specific timepoints to promote regenerative tendon healing.

Title: **Unilateral and bilateral ACL injuries exhibit distinct sensitivity of chondrocytes to injurious impact loading.**

Presenting Author: Alexander Kotelsky

Co-Authors: Ashley Proctor, Anissa Elahi, Nejat Yigit Can, Sandeep Mannava

Lab PI / Mentor: Whasil Lee

Abstract (3500 characters or 500 words Limit)

Anterior cruciate ligament (ACL) tears destabilize knee joints and alter gait kinematics. The resulting aberrant mechanical loading may cause injury/death of articular chondrocytes, promote imbalanced metabolism, and eventually develop post-traumatic osteoarthritis (PTOA). In this study, we investigate the extent to which alterations in in-vivo loading environments impact the sensitivity of chondrocytes to injurious loading in ACL-injured knees in both males and females. To this end, we used non-invasive unilateral (uni-ACL-I) and bi-lateral (bi-ACL-I) ACL injury mouse model in order to test hypotheses that (1) bi-ACL-I will induce a higher uncompensated loading on injured limbs, and (2) this gait loading will increase sensitivity of chondrocytes to injurious mechanical impacts in mice as compared to uni-ACL-I, where the gait pattern may be compensated for by the un-injured limbs.
Knee joints of 8-9 week old male/female C57BL/6 mice were subjected to an axial force in a flexed position until a “pop” sound was heard. The resulting ACL-rupture was confirmed by Lachman and Drawer tests indicating an increased joint laxity. The alterations in mouse gait due to ACL-I were assessed using the Noldus CatWalk XT system at 2, 4 and 8 weeks post-injury. Interestingly, while female bi-ACL-I mice exhibited a consistently higher contact intensities in their hindlimbs at each timepoint post-injury, male bi-ACL-I mice showed a non-significantly elevated contact intensity at 2-week timepoint followed by intensity levels similar to uni-ACL-I and uninjured controls at 4- and 8-week timepoints. To assess the effect of ACL-I type on sensitivity of articular chondrocytes to injurious impacts, carefully dissected distal femurs with intact cartilage from mice sacrificed at 0-,4-, and 8-week post-injury were vitally stained, placed on a cover glass and subjected to 1mJ impacts, such that cartilage on femoral condyles was compressed against the glass resulting in injured/dead cells. Areas of injured cells on lateral condyles were quantified. While the uni-ACL-I joints had larger areas of injured cells at 0-week post injury, they exhibited similar levels of mechano-vulnerability as uninjured contralateral limbs at 4- and 8-week post injury in both male and female mice. In contrast, the bi-ACL-I exhibited increased cell vulnerability as compared to controls over the course of the experiments. Additionally, there was no difference in cell vulnerability between injury types (uni-ACL and bi-ACL) at 0-week post injury presumably caused by post-traumatic knee joint inflammation in both female and male mice. However, compaired to uni-ACL-I cell vulnerability in the bi-ACL group was higher at 4- and 8-week time points in female mice, and only at 4-week post-injury time point in male mice. Surprisingly, only bi-ACL-I revealed gender-related difference in cell vulnerability at 8 weeks post injury.
Taken together, our findings revealed that bi-ACL-I increases both gait-associated mechanical loading on injured limbs and the cellular mechano-vulnerability to impact loads, which may contribute to faster PTOA pathogenesis. Interestingly, uni-ACL-I was able to compensate for the gait and reach levels of max gait intensity as well as cell vulnerability similar to uninjured controls. Future research will investigate more in-depth the altered physiology of articular chondrocytes, mechanical properties of the extracellular matrix, as well as PTOA progression due to ACL-I.

Title: **Targeting synovial lymphatic function as a novel therapeutic intervention for osteoarthritis**

Presenting Author: Xi Lin

Co-Authors: H. Zhang, R.D. Bell, J.H. Jonason, E.M. Schwarz, B.F. Boyce, L. Xing

Lab PI / Mentor: Lianping Xing

Abstract (3500 characters or 500 words Limit)

Osteoarthritis (OA) is the major cause of disability in the elderly with no effective cure. While it is known that OA involves articular cartilage catabolism, how catabolic factors are removed from joints during homeostasis and OA progression has not been studied. Previously, we reported the importance of the synovial lymphatic system (SLS) in the pathogenesis and treatment of inflammatory/erosive arthritis in mice. These studies showed that the SLS consists of lymphatic capillaries in the synovium, collecting lymphatic vessels (LVs), and the draining lymph nodes (DLNs). Lymphatic endothelial cells (LECs) and lymphatic muscle cells are two major cell types of the LVs. Vascular endothelial growth factor C (VEGF-C) and signaling through its receptor, VEGFR3 are crucial for LEC development, survival and migration. In the current study, we aimed to investigate the involvement of the SLS in age-related OA, and tested the hypotheses that: 1) aged mice have impaired SLS function due to dysregulated VEGF-C/VEGFR3 signaling; and 2) improvement of the SLS through VEGF-C administration will reduce OA tissue damage in aged mice. To determine whether lymphatic drainage is decreased in aged knees, we examined the SLS functions using IVIS-Dextran lymphatic imaging in knee joints of 3-m and 19-m mice. 19-m old mouse knees had lower joint clearance (19-m 54.0±4.2% vs. 65.3±3.6% in 3-m, $p<0.05$). Transmission electronic microscopy demonstrated abnormal ultra-structure in 19-m mouse LVs with thinner endothelium, pronounced vacuolization, and blebbing. We also confirmed osteoarthritic changes in the knees of the same cohort of 19-m old mice. To explore the potential mechanisms of age-related SLS dysfunction, we performed bulk RNA sequencing using synovial tissues of 3-m and 24-m old mice. Markedly different transcriptome profiles were present between 3-m and 24-m samples. The expression of genes associated with lymphangiogenesis was decreased in 24-m synovium, including the LEC growth factor Vegf-c, which was confirmed by qPCR. Since VEGF-C signals VEGFR3, a member of transmembrane receptor tyrosine kinase, we examined the expression levels of genes involved in the receptor protein tyrosine kinase signaling pathway. Impressively, the majority of genes in this pathway were downregulated in 24-m mice. To test if decreased VEGF-C contributes to age-related SLS dysfunction and OA, we treated 19-m old mice with VEGF-C or Veh for 12 wks. VEGF-C treatment improved SLS function, indicated by increased joint clearance (VEGF-C 63.2±9.1% vs. 52.5±15.2% in Veh, $p<0.05$). Histomorphometry analysis of Safranin-O-stained slides (VEGF-C 38.1±7.3 mm2 vs. 25.7±6.9 mm2 in Veh, $p<0.05$) revealed that VEGF-C increased cartilage area and decreased osteophyte area (VEGF-C 8.0±5.3 mm2 vs. 14.6±7.3 mm2). In addition, microCT revealed that VEGF-C decreased calcified meniscus (VEGF-C 15.7±1.3 mm2 vs. 19.0±3.9 mm2 in Veh, $p<0.05$) and subchondral trabecular bone area (VEGF-C 30.6±1.7 mm2 vs. 37.2±7.7 mm2 in Veh, $p<0.05$), indicating VEGF-C reduced age-related OA progression. In conclusion, we showed that VEGF-C/VEGFR3 signaling is essential for LV homeostasis, and its dysfunction in the synovium contributes to age-related OA. Targeting SLS synovial lymphatic function by improving VEGF-C signaling presents a novel therapeutic intervention for OA.

Title: **Age-associated callus senescent cells produce TGF beta1 that inhibits bone fracture healing in aged mice**

Presenting Author: Jiatong Liu

Co-Authors: Hengwei Zhang, Brendan F. Boyce

Lab PI / Mentor: Lianping Xing

Abstract (3500 characters or 500 words Limit)

Cell senescence plays important roles in human diseases, and clearance of senescent cells (SCs) prevents age-related bone loss and joint damage. SCs produce the senescence-associated secretory phenotype (SASP) to affect the function of target cells. Delayed fracture healing is common in the elderly, which is accompanied by reduced mesenchymal stem/progenitors (MPCs). However, the contribution of cell senescence to aged fracture healing remains to be studied. Previously, we found that the senolytic drugs, dasantinb + quercetin, enhanced fracture healing in aged, but not in young mice, and conditioned medium (CM) collected from aged callus inhibited the growth of callus-derived MPCs (CaMPCs), indicating a potential role of SCs in aged fracture healing. To detect critical SASP factors produced by aged callus SCs, we examined the expression levels of 22 SASP factors including TGF beta, pro-inflammatory cytokines, chemokines, and MMPs. Compared to young callus tissues, TGF beta 1 was the most elevated SASP factor in aged callus tissues (by 11-fold over young) as well as in purified callus p16+ SCs (by 23-fold over young). Thus we hypothesize that callus SCs in aged mice produce excessive TGF beta 1, which inhibits the proliferation of CaMPCs and delays fracture healing, and this can be prevented by TGF beta neutralization. To test our hypothesis, we used 3-m-old C57BL/6J as young and 19-m-old as aged mice and examined the expression pattern of senescent genes, p16 and p19 in callus tissues at different days post tibial fracture (dpf) surgery by qPCR. Compared to young mice, callus tissues from aged mice expressed high levels of p16 and p19, which peaked 10 dpf, a time when soft callus has formed and declined 21 dpf (remodeling phase). Using CM collected from callus harveted at 10 dpf, the time when the expression of senescent genes is high, we found that aged callus CM decreased the area of methylene blue+ cells (=growth 11±1 vs. 24±2 mm*2 in young callus CM) and BrdU+ cells (=proliferation, 5±0.4 vs. 14±2.6% in young callus CM). 1D11, a pan TGF beta neutralizing Ab that blocks TGF beta 1-3, significantly reduced the inhibitory effect of aged callus CM on the growth and proliferation of CaMPCs more than cells treated with IgG (methylene blue+ area: 27±4 vs. 11±1 mm*2 in IgG; BrdU+: 8±1 vs. 3±1% in IgG). Finally, we treated aged mice with 1D11 or isotype IgG1 Veh by intra-callus injection at 1, 3, 5, and 7 dpf. Mice were sacrificed at 10 dpf and calls tissue were subjectedd for histology and flow cytometry. 1D11 significantly increased the callus volume (3±0.5 vs. 2±0.5 mm*3 in Veh), new bone area (0.4±0.1 vs. 0.3±0.07 mm*2 in Veh), and cartilage area (0.3±0.03 vs. 0.2±0.03 mm*2 in Veh), which was accompanied by increased Ki67+ proliferating cells (6±0.7 vs. 4±1.2% in Veh) and callus CD45-CD31-CD105+ MPCs (4.9±0.2 vs. 3.7±0.3% in Veh). More importantly, this TGF beta neutraling significantly increased bone stiffness (752±212 vs. 359±101 N.mm/(rad/mm) in Veh), bone strength (22±3.5 vs. 17±2.0 N.mm in Veh), and bone toughness (0.22±0.06 vs. 0.13±0.01 N.mm*/(rad/mm) in Veh) at 35 dpf. Thus, our study demonstrate TGF beta1 as an important SASP factor that is produced by callus SCs in aged mice and inhibits MPC proliferation. Local blockade of TGF beta signaling during the early phase of fracture healing may represent a new therapeutic strategy for fracture healing in the elderly.

Title: **Multiphoton microscopy with clearing for three dimensional histology of mouse digital flexor tendon**

Presenting Author: Melissa MacLiesh

Co-Authors:

Lab PI / Mentor: Hani Awad / Michael Giacomelli

Abstract (3500 characters or 500 words Limit)

Injuries to digital flexor tendons are prone to forming fibrotic adhesions, which severely impair the function of the hand. We have developed a mouse model of digital flexor tendon healing in mice. Histological analysis is typically required to view the microscopic anatomy of the injured tissue and is performed by slicing the tissue into thin sections and observing under a microscope. Traditional sectioning of extremely thin samples, such as mouse digital flexor tendon, has proven difficult to capture the injury site in its anatomical context due to their small size. Sectioning is also susceptible to tearing and folding and offers limited 2D information. Reconstructing the 2D information into a 3D volume of the tissue is time consuming and difficult. With the advent of tissue clearing, it is possible to render large biological samples transparent, increasing the penetration depth of light into the sample. This enables multiphoton microscopy to optically section thick samples in real time, creating a z-stack, which can be easily reconstructed in 3D. The goal of this project is to provide a reliable method for 3D virtual histology of the digital flexor tendon and injury site, capable of providing both fine details at the cellular level and a big picture perspective at the tissue level. In this study, we evaluated three clearing methods: BABB (benzyl alcohol benzyl benzoate), PEGASOS (polyethylene glycol (PEG)-associated solvent system), and CUBIC (clear unobstructed brain imaging cocktails). Each method was able to render a mouse paw translucent in 5, 12, and 14 days respectively. The paws were stained with fluorescent dyes methyl green (nuclear) and eosin yellow (counter). Additionally, we compared wound healing between WT and MRL/MpJ mice over 28 days following injury. MRL/MpJ mice have been noted to have an accelerated regenerative potential and the comparison against WT mice functions both as a proof of concept that our model can capture the 3D tendon injury site in detail, and also to highlight the changes in WT injured tendon vs the nearly scarless MRL/MpJ model. Using a custom built two-photon microscope, we were able to image the cleared mouse paws and view the deep digital flexor tendon in the digits of interest up to a depth of 500μm until the signal was lost in bone. The images were captured with less than 500nm lateral and 6μm axial resolution, enabling visualization of the tendon matrix, and highly aligned tenocyte nuclei. We were able to identify both superficial digital flexor tendons, the deep digital flexor tendon, and the structurally supportive retinacula. The retinacula are fibrous connective tissue components, notably less organized than the collagen fibrils of tendon, which run perpendicular to the digital flexor tendon. We have also demonstrated the compatibility of this clearing method with second harmonic generation (SHG) imaging of the collagenous organization of the matrix, which will allow us to quantitatively assess the disorganized scar tissue in the injured tendon. We are also planning to assess the compatibility of this clearing approach with immunohistochemistry and fluorescent reporter mice. In conclusion, this tissue clearing approach can produce image quality comparable to traditional histology without the need for sectioning. It offers histologic data in the 3-dimensional context of the tissue and has the potential to transform the way we assess musculoskeletal tissues response to injury.

Title: **Sex Differences in Age-Related Changes to Bone in the Senescence-Accelerated Mouse Prone 8 (SAMP8) model**

Presenting Author: Christine Massie

Co-Authors: Emma Knapp, Keren Chen, Andrew Berger, Hani Awad

Lab PI / Mentor: Hani Awad

Abstract (3500 characters or 500 words Limit)

Senescence-accelerated mouse (SAM) is a commonly used model for studying aging-related functional declines. SAMP6 is a well-characterized model for studying senile osteoporosis, whereas SAMP8 is a model for impaired learning, memory, and immune response. We hypothesized that the female SAMP8 mouse could experience osteoporosis during accelerated senescence and aging. 18 female, 18 male SAMP8 mice were included in the study at ages 11-52 weeks. Dual energy X-ray absorptiometry (DXA) was performed in vivo. Femurs and tibias were excised after animal sacrifice and tibias were evaluated by ex vivo DXA, micro-computed tomography (μCT), Raman spectroscopy, and biomechanical testing (torsion testing) and femurs were evaluated by ex vivo μCT. 18 female and 18 male SAMR1 mice were also evaluated similarly. We observed many multimodal bone properties had a significant effect due to sex when a three-way ANOVA was performed. To focus on sex differences, we kept the SAMP8 and SAMR1 datasets separate and analyzed the data with analysis of covariance (ANCOVA) with age set as a covariate term ($p<0.05$ significance criterion). In vivo DXA measurements showed that females significantly increased whole body bone mineral density (BMD) over age relative to males, which did not significantly change over range of ages evaluated. This trend was not seen in SAMR1, as sex was not a significant factor. The tibial and femoral midshaft cortical thickness showed males significantly decreased with age relative to females, who slightly increased with age. In SAMR1, both sexes significantly decreased with age. The SAMR1 showed both sexes significantly decreased with age in femoral cortical thickness. We also evaluated the trabecular bone in the femoral head and neck using ex vivo μCT. In the femoral head, we observed decreases in trabecular number (Tr.N) and increases trabecular spacing (Tr.Sp) with age in the SAMP8 females and males. We also evaluated the trabecular bone in the femoral head and neck using ex vivo μCT. In the femoral head, we observed decreases in Tr.N and increases Tr.Sp with age in the SAMP8 females and males. We observed that both sexes in SAMP8 slightly increased in trabecular thickness (Tr.Th). However, in the SAMR1 mice both sexes significantly decreased Tr.N and significantly increased Tr.Sp and Tr.Th with age. Biomechanically, we observed that torsional rigidity significantly increased with age in both sexes in both cohorts. We observed no significance with maximum torque in SAMP8 mice, but in SAMR1, males significantly increased with age relative to females. Ex vivo Raman spectroscopy measurements of the tibial midshafts revealed no significant differences with sex or age for the mineral to matrix ratio (phosphate/amide I) while crystallinity significantly decreased with age in both sexes in SAMP8. Conversely, SAMR1 had a significant decrease in mineral to matrix ratio in both sexes, but no significant change with age in crystallinity. The results indicate that the SAMP8 murine model does not display consistent features of senile osteoporosis over the age span examined but there are intriguing sex differences with age. One limitation in this study is that the old cohort represents the midlife of the SAMR1 but is closer to end of life in the SAMP8 mice. This confounds our ability to examine true aging effects on bone health. Future studies will examine sex- and age- related changes in femoral neck strength in SAMP8 and SAMR1 mice.

Title: **Vasculotropic and Osteotropic Features of S. agalactiae vs. S. aureus Implant-Associated Bone Infection in Mice**

Presenting Author: Elysia A Masters

Co-Authors: Stephanie P Hao, H. Mark Kenney, Yugo Morita, Karen L de Mesy Bentley, Chad A Galloway, Benjamin F Ricciardi, Edward M Schwarz and Irvin Oh, MD

Lab PI / Mentor: Edward M Schwarz and Irvin Oh, MD

Abstract (3500 characters or 500 words Limit)

Osteomyelitis, defined as bacterial infection of bone, remains a devastating complication of orthopaedic surgery. The most common pathogens isolated from periprosthetic joint infections (PJI) include Staphylococcus aureus (S. aureus) and Group B Streptococcus (GBS, S. agalactiae). Clinically, S. aureus PJI is associated with local inflammation, abscesses and aggressive osteolysis, while S. agalactiae PJI is generally associated with soft tissue damage and vascular spread. Preclinical models of S. aureus implant-associated infection have proven useful, however no animal models of S. agalactiae osteomyelitis exist. Here, we aimed to develop a murine model of S. agalactiae PJI based on a well-established S. aureus model of implant-associated osteomyelitis and compare differences in microbial pathogenesis.

All animal studies were performed in accordance with protocols approved by the University Committee on Animal Resources at the URMC. Surgery was performed as previously described4. Briefly, 6-week-old, female Balb/C mice were anesthetized with xylazine (12 mg/kg) and ketamine (130 mg/kg) and administered preoperative slow-release buprenorphine. Stainless-steel pins were sterilized, then inoculated with either S. aureus (USA300) or S. agalactiae (COH1) for 20 minutes (approximately 5.0 x 10^5 CFU/mL) and implant through the tibiae. Animal weight was tracked, and X-ray imaging was performed at day 0 and 14. Tibiae were harvested at day 14 post-infection for CFU quantification (n > 8), μCT imaging (n = 5), histology (n = 3) and TEM (n = 3).

S. agalactiae-infected animals were significantly heavier than S. aureus-infected animals at days 6, 8, and 14 post-infection. Quantification of CFU's at day 14 post-infection revealed that S. agalactiae infections had undetectable CFUs on the implant, and fewer within soft tissue and bone, compared to S. aureus infections. S. agalactiae induced significantly less peri-implant osteolysis compared to S. aureus, by measurement of pin hole volume from μCT scans. Histologic staining for TRAP confirmed that S. agalactiae induces significantly fewer osteoclasts on cortical bone surfaces versus S. aureus. H&E and Brown-Brenn staining showed that while S. agalactiae does not form abscesses like S. aureus, both pathogens successfully colonize bone sequestra. TEM of infected bone fragments revealed that S. aureus invades and colonizes the osteocyte-lacuno canalicular network (OLCN), noted by bacteria within the submicron-sized canaliculi. On the other hand, S. agalactiae colonizes blood vessels embedded within bone, noted by bacteria within the large diameter vessels alongside multi-nucleated immune cells. Finally, both pathogens are capable of degrading mineralized bone matrix, as evidenced by scalloping of bone surrounding bacteria.

Clinical and experimental studies of PJI have determined the major reservoirs of S. aureus persistence in osteomyelitis. Here we show that S. agalactiae does not colonize the implant hardware or form bone marrow abscesses, resulting in less peri-implant osteolysis and implant loosening. Interestingly, S. agalactiae preferentially colonizes the vasculature within bone, as evidenced by TEM imaging of infected bone. Taken together, S. agalactiae infects as a vasculotropic pathogen, relative to the osteotropic behavior of S. aureus, during the establishment of implant-associated osteomyelitis. Additionally, we are the first to describe S. agalactiae-mediated bone degradation.

Title: **A unique B cell population revealed by single cell RNA analysis of the RA synovium**

Presenting Author: Nida Meednu

Co-Authors: Andrew McDavid, Javier Rangel-Moreno, Katherine Escalera-Rivera, Jennifer Albrecht

Lab PI / Mentor: Jennifer H Anolik

Abstract (3500 characters or 500 words Limit)

Background: Ectopic lymphoid structures (ELS) have been observed in synovial tissue of rheumatoid arthritis (RA) patients but their functional relevance in the disease remains unclear. Additionally, little is known about B cell activation pathways during ectopic lymphoid neogenesis (ELN). In this study, we utilized single cell RNA sequencing coupled with B cell repertoire sequencing to characterize B cell subsets that may play a role in ELN in RA synovial tissue and support local B cell activation and development of autoreactive plasma cells.
Methods: Synovial tissue was selected based on the presence of lymphocytic infiltrates by histology (n=4 RA patients). Tissue was disaggregated using protocols established by the Accelerating Medicines Partnership (AMP) consortium. scRNA-seq was performed on sorted tissue B cells using the 10x genomic platform with poly-A selected, 5' initiated expression and V(D)J libraries generated from each single cell. Transcriptomic clusters were compared using supervised classification techniques to AMP phase I RA synovial B cells (n=10), SLE kidney B cells, and blood B cells. Combined single cell repertoire/RNA sequencing from an additional 13 RA synovial samples and 10 matched blood B cells are currently under analysis in AMP phase II. In vitro studies were conducted for elucidation of signals promoting in situ B cell activation, with NR4A detected by qPCR and flow cytometry.
Results: Using single cell RNA sequencing analysis, we identified a unique B cell subset in the RA synovium characterized by high expression of NR4A1-3, a family of orphan nuclear receptors (NUR77, NURR1, and NOR1) that are induced by acute and chronic antigen stimulation in lymphocytes and function as ligand-independent transcription factors. The NR4A+ B cell cluster showed evidence of somatic hypermutation (SHM) and class-switched recombination based on repertoire analysis. The rate of SHM was positively correlated with NR4A1 and NR4A2 gene expression and inversely correlated with IGHD gene expression. Gene Set Enrichment Analysis revealed that the NR4A+ cluster has a transcriptomic profile between naïve and germinal center (GC) B cells sorted from tonsil and differentially expressed genes characteristic of GC centrocytes including CD83 and GPR183. In SLE kidney, and peripheral blood B cells, NR4A+ B cells were reduced to 0.7% and 1.5% abundance, respectively, compared to >40% abundance in synovial tissue from AMP phase I and the 10X platform ($p<0.001$ under logistic mixed models). NRA4 was upregulated at both the RNA and protein level upon activation through the B cell receptor in vitro. NR4A1 protein was expressed spontaneously in RA tissue B cells by flow cytometric and histologic analysis.
Conclusions: Our data suggest a dynamic progression of B cell activation in RA synovial ectopic lymphoid structures, with NR4A a potential read-out of chronic antigen activation and local adaptive immune responses.

Title: **Multiaxial and multiscale strain assessment of the impinged mouse Achilles tendon insertion**

Presenting Author: Keshia Mora

Co-Authors: Samuel Mlawer

Lab PI / Mentor: Mark Buckley (PI) and Alayna Loiselle (co-PI)

Abstract (3500 characters or 500 words Limit)

Introduction: Mechanical deformation applied at the tissue-scale is transferred to the microscale—including the local extracellular matrix, the pericellular matrix (PCM), the cell and the nucleus—through a process known as strain transfer. Microscale strains, in turn, trigger biological activity that plays an important role in the maintenance of tendon phenotype and homeostasis. Although tendon predominantly experiences tensile forces, impingement has been implicated in both physiological (i.e., formation and homeostasis of the tendon insertion) and pathophysiological processes (i.e., rotator cuff tendinopathy and insertional Achilles tendinopathy). Therefore, the objective of this study was to assess the micromechanical strain environment in the impinged Achilles tendon insertion. We hypothesized that impingement would generate transverse compressive strain at the matrix, PCM and cell scales.

Methods: Hindlimb explants of 12-16 week old C57BL/6J (N=7) mice were harvested and stained with Hoechst, fluorescein diacetate and propidium iodide to visualize tenocyte nuclei and intracellular space, and to assess cell viability. Following, explants were loaded into a custom-built platform consisting of a grip and 3-D printed based plate that fit inside a plexiglass box filled with media. A cord tied around the mouse paw was pulled in order to enable passive dorsiflexion (upward ankle rotation) of the paw from an angle of 165° (initial position) to 125° (final position); thereby inducing impingement of the Achilles tendon insertion. Explants were imaged on a multiphoton microscope, and image stacks of the same population of tenocytes were obtained at the Achilles tendon insertion (1 mm from the calcaneus) before and after passive dorsiflexion. Local matrix strain was quantified by assessing the Green-Lagrange strain tensor based on the changes in the position of tracked cells. While PCM strain was quantified based on the cell-cell gap distance. Cell deformation was quantified based on the cell strain as well as changes in cell aspect ratio.

Results: Our data demonstrate that at the matrix-scale, impingement generated large transverse compressive strains (-19.8%) along the z-axis (direction of impingement). In addition, large compressive strain (-13.6%) were observed along the y-axis of the tendon, and relatively small tensile strains (1.3%) were observed along the x-axis (direction of collagen alignment). At the PCM-scale, there was substantial compression of the PCM (-27%). While at the cell-scale there was an increase in cell aspect ratio ($p = 0.47$), as well as tensile strains (8.3%) observed along the x-axis.

Discussion: This study was designed to characterize the micromechanical strain environment in the impinged Achilles tendon insertion. Our findings demonstrate that impingement generates substantial matrix-scale compressive strains, leading to compression of the tendon PCM and a significant increase in cell aspect ratio. Since microscale mechanical deformations are a key step in the chain of events leading from impingement to biological output, our findings shed light on the microscale mechanical changes that are likely to influence the biological sequelae of impingement. Understanding the factors that influence the microscale strain environment could contribute to a more detailed mechanistic understanding of impingement-induced tendinopathies and inform the development of approaches that disrupt the progression of pathology.

Title: **IL-27 suppresses Staphylococcal abscess formation in Staphylococcus aureus implant-associated osteomyelitis**

Presenting Author: Yugo Morita

Co-Authors: Stephen L. Kates, John R. Owen, John L. Daiss, Edward M. Schwarz and Gowrishankar Muthukrishnan

Lab PI / Mentor: Edward M. Schwarz and Gowrishankar Muthukrishnan

Abstract (3500 characters or 500 words Limit)

INTRODUCTION: Currently, the role of IL-27 in S. aureus surgical-site infection (SSI) is unknown. To better understand this, we tested the hypotheses that IL-27: 1) is elevated in patients with S. aureus orthopaedic infections, and 2) improves bacterial clearance after S. aureus SSI in mice.
METHODS: Clinical study (IL-27 Luminex assay): Serum samples were collected from S. aureus osteomyelitis patients, patients who succumbed to septic death after S. aureus osteomyelitis , and healthy controls, following informed consent on IRB-approved protocols. Serum cytokine levels, including IL-27, were determined via Luminex assay. Vertebrate animals: All studies with mice were performed on IACUC-approved protocols. In vitro reactive nitrogen species assay: Primary bone marrow-derived murine macrophages were pretreated with PBS or IL-27 for 24 hours, and then stimulated with LPS in the presence or absence of IL-27 for 24 hrs. Nitric oxide (NO-) concentration in the culture supernatants was determined via the Griess reaction assay, and differences between groups were determined by ANOVA. In vivo S. aureus implant-associated osteomyelitis experiment: C57BL/6 mice were injected intramuscularly with recombinant adeno-associated virus (rAAV) expressing IL-27 or GFP (control). All mice were challenged with a MRSA contaminated trans-tibial implant. Animal weight and BLI were obtained on days 0, 1, 3, 7, 10 & 14, and CFUs on the implant and surgical site tissue were determined after euthanasia on day 14 post-op.
RESULTS: IL-27 was significantly elevated in the S. aureus osteomyelitis patients compared to healthy controls ($p<0.001$). Moreover, serum IL-27 levels immediately following septic death from S. aureus osteomyelitis were 20-fold greater than that of healthy control patients ($p<0.0001$). Next, we evaluated the effects of IL-27 signaling on the induction of reactive nitrogen species formation in macrophage cultures. The results showed that IL-27 alone had no effect on NO- formation. However, combination of IL-27 and LPS stimulation increased NO- production over LPS activation alone ($p<0.0001$), suggesting a costimulatory effect. In vivo, rAAV-IL-27 treated mice showed significantly greater body weight recovery compared to rAAV-GFP treated mice ($p<0.01$ on on days 10 & 14 post-op). Remarkably, rAAV-IL-27-treated mice showed much smaller draining abscesses compared to the rAAV-GFP control group. While no differences in CFU were found on the implants on day 14, the bacterial load in the adjacent tissues was significantly lower in the rAAV-IL-27-treated mice ($p<0.01$).
DISCUSSION: S. aureus osteomyelitis remains a major healthcare burden, and the host factors that impact outcome are poorly understood. Here we show that there is a significant association between IL-27 serum cytokine levels and S. aureus osteomyelitis. Preclinically, we demonstrated that IL-27 stimulates macrophage differentiation towards M1 and it is a co-stimulator with TLR signaling to increase reactive nitrogen species production by macrophages in vitro. We also showed that mice with increased IL-27 levels have ameliorated S. aureus implant-associated osteomyelitis. Thus, IL-27 appears to be protective.
SIGNIFICANCE: Our data indicates that IL-27 could be having a proinflammatory phenotype causing dramatic suppression of Staphylococcal abscess formation due to S. aureus osteomyelitis. Drugs that induces IL-27 expression could be potential treatments for S. aureus osteomyelitis.

Title: **Blunted CCR2 and macrophage recruitment impedes functional recovery during tendon healing**

Presenting Author: Samantha Muscat

Co-Authors: Emma Gira

Lab PI / Mentor: Alayna Loiselle

Abstract (3500 characters or 500 words Limit)

Recruitment of macrophages is a critical component of the inflammatory phase of tendon healing. Macrophages play key roles in mediating fibroblast proliferation and extracellular matrix deposition. Monocyte chemoattractant protein -1 is the primary ligand for the chemokine receptor 2 (CCR2) and mediates macrophage infiltration into tissues during injury.Thus, CCR2 represents an ideal target to define the role of circulating macrophages during pathologies such as tendon healing. The role of CCR2, and thereby extrinsic macrophages, in tendon healing remains unknown. There is clear evidence that extrinsic macrophages can modulate the cellular environment, particularly myofibroblasts, in many tissues. In the present study, we tracked the infiltration and retention of CCR2+ extrinsic macrophages, and defined the functional effects of CCR2-/- on tendon healing and myofibroblast differentiation. We tested the hypothesis that CCR2-/- would blunt macrophage recruitment, and therefore myofibroblast differentiation, resulting in a reduction in biomechanical properties following acute tendon injury and repair.

CCR2GFP/+ mice have green fluorescent protein inserted into the chemokine receptor 2 gene, resulting in expression of eGFP and CCR2 in hemizygous mice. CCR2GFP/GFP results in a loss of function and therefore loss of macrophage recruitment. CCR2+/+ have normal CCR2 expression and are used as wildtype (WT) controls. The University Committee on Animal Resources approved all animal studies. 10-12 week old male and female CCR2GFP/GFP and CCR2+/+ mice underwent complete transection and surgical repair of the flexor digitorum longus tendon. Hind paws were harvested for gliding and biomechanical analyses. All samples were harvested for routine de-calcified histology and sagittal sectioning to assess the eGFP signaling. Myofibroblasts were identified by immunofluorescence using a α-SMA-Cy3 antibody.

Early recruitment of CCR2+ was observed by D3 post-surgery, with these cells seen through at least D21, indicating persistence of these cells after resolution of acute inflammation. At D8 we see greater myofibroblast retention in WT than CCR2 GFP/GFP mice. Later, at D28 we still see this difference. There were no differences in mechanical properties observed between WT and CCR2-GFP/GFP mice at D14, in contrast to other anti-inflammatory approaches, which typically impair early healing. By D28, there was a significant reduction in Max load at failure ($p=0.03$) and stiffness ($p=0.05$) of CCR2GFP/GFP, relative to WT. These data indicate that inhibited CCR2+ cell recruitment impedes functional recovery post-injury during the later phases of healing, after resolution of acute inflammation. While there was a reduction in CCR2GFP cells in CCR2GFP/GFP compared to CCR2 GFP/+, this model does not completely inhibit recruitment of CCR2+ cells. Future work characterizing what other cell populations are regulating and recruiting CCR2+ macrophages need to be investigated. CCR2GFP/GFP impacts late healing, suggesting that these cells may also have inflammation-independent functions. Understanding their time-dependent functions during healing will be important. Since macrophages drive fibrosis, understanding the cellular and functional outcomes of impaired monocyte/ macrophage recruitment is necessary for the development of future therapeutic strategies.

Title: **Identification and characterization of a genetic marker for epitenon cells**

Presenting Author: Anne E.C. Nichols

Co-Authors: Keshia E. Mora, Alayna E. Loiselle

Lab PI / Mentor: Alayna Loiselle

Abstract (3500 characters or 500 words Limit)

Tendon injuries are common and heal poorly, often through the formation of adhesive scar tissue that limits tendon functionality. It has traditionally been thought that healing which occurs through the contributions of intrinsic tendon cells (those derived from the tendon parenchyma, epitenon/endotenon) is superior to healing that occurs mainly through the action of cells extrinsic to the tendon. Though tremendous progress has been made in identifying and characterizing the roles of various resident cell populations within the tendon body (Scleraxis [Scx]-lineage, S100a4-lineage) or tissues adjacent to the tendon, including the sheath (TPPP3-lineage) through the use of genetic mouse models, there is currently no marker for epitenon cells which severely limits our understanding of how these cells contribute to tendon homeostasis and repair. In the present study, we identified GLAST-CreERT2 as a novel Cre driver that specifically labels epitenon cells (GLAST-lineage [lin]), an epithelial-like cell population located on the surface of the tendon, in adult mice and that can be used to trace this population of cells during healing. As epithelial cells are known to play a crucial role in restoring tissue integrity during early wound healing in other tissues, we hypothesized that GLAST-lin epitenon cells would localize to the bridging scar tissue that forms following acute injury of the flexor digitorum longus (FDL) tendon. To facilitate tracing of GLAST-lin epitenon cells, GLAST-CreERT2 mice were crossed to the ROSA-Ai9F/F reporter strain (GLAST-CreERT2; Ai9F/F). In order to better understand the relationship between GLAST-lin cells and Scx-expressing tendon cells, GLAST-CreERT2; Ai9F/F mice were crossed to the Scx-GFP strain. A combination of immunofluorescent staining and multiphoton imaging were then used to evaluate the localization of GLASTAi9 cells during tendon homeostasis and healing. GLASTAi9 cells are located outside the collagen matrix of the tendon body and form a single-cell thick layer on the surface of intact tendons. GLAST-CreERT2 also labels a very small subset (<1%) of Scx-GFP+ tenocytes located within the FDL tendon parenchyma. Future studies will determine whether the GLASTAi9 cells located with the tendon proper are labeled in situ or are labeled in the epitenon prior to their migration into the tendon where they subsequently turn on Scx expression. If GLASTAi9 epitenon cells begin to express Scx upon migration to the tendon body, this may identify GLASTAi9 cells as a tendon progenitor cell population. Following injury, GLASTAi9 cells proliferate locally within the epitenon at day 10 and form a thickened, cellular capsule around the scar area by day 14 which persists through at least day 28 post-repair. GLASTAi9 cells are found both within the bridging scar tissue occupied by Scx-GFP+ cells as well as in a discrete band of GLASTAi9 cells adjacent to the Scx-GFP+ cell bridge. Though the majority of GLASTAi9 cells located within the repair area are not Scx-GFP+, a few GLASTAi9; Scx-GFP+ cells are found both within the tendon stub as well as within the bridging scar tissue. Ongoing cell depletion and fate mapping studies will further define the role of GLASTAi9 epitenon cells in flexor tendon homeostasis and repair.

Title: **Assessment of Standard of Care Antibiotic Therapies to Eradicate Staphylococcus aureus Occupying the Osteocyte-Canalicular Network of Cortical Bone in a Transtibial Implant Model of Osteomyelitis**

Presenting Author: Mark J. Ninomiya, MS

Co-Authors: Elysia A. Masters, MS; Karen L. de Mesy Bentley, MS; Edward M. Schwarz, PhD

Lab PI / Mentor: Edward M. Schwarz, PhD

Abstract (3500 characters or 500 words Limit)

INTRODUCTION: In prosthetic joint infections (PJI), S. aureus is able to persist within the bone adjacent to the implant, which requires invasive revision surgeries and is associated with an increased patient mortality. One potential mechanism for S. aureus's persistence in PJIs is its ability to invade and colonize the osteocyte-lacuno canalicular network of cortical bone (OLCN) at the infection site. Although it is known that parenteral small molecule drugs can enter the OLCN, the susceptibility of S. aureus within this protected environment to standard of care surgical interventions and antibiotic regimens remains unclear and warrants further investigation.

METHODS: Animal studies were performed on IACUC-approved protocols (UCAR 2003-164E). We utilized an established murine model of PJI that mimics clinical antibiotic therapy (1). Briefly, female BALB/cJ mice are purchased at six weeks of age and then acclimated in their housing room for one week prior to surgery. Mice are administered a 72-hour slow-release buprenorphine subcutaneously (sc) and then anesthetized with a combination of ketamine and xylazine injected intraperitoneally (ip). The surgical site is exposed by a lateral approach followed by blunt dissection. After the tibia is debrided of superficial tissue, an L-shaped stainless-steel pin, which has been soaked for 20 minutes in an overnight culture of bioluminescent (BLI) S. aureus, is inserted trans-cortically into the tibia via a medial-to-lateral implantation. Once the implant has been placed, the soft tissue surrounding the tibia and skin are closed. Following inoculation surgery, correct hardware placement is assessed by planar X-ray. From day seven to fourteen post-infection surgery, mice are administered systemic antibiotic therapy and then harvested for colony-forming units (CFU) assays and transmission electron microscopy (TEM) imaging. BLI is measured over the 14-day time course to measure bacterial proliferation in vivo.

RESULTS: Unexpectedly, nafcillin and gentamicin antibiotic treatments showed no significant effect versus the placebo on reducing methicilin-sensitive S. aureus (MSSA) growth in vivo via BLI or CFU counts on the tissues and implants. Similarly, vancomycin has littile effect on methicilin-resistant S. aureus (MRSA) osteomyelitis. TEM studies are in progress.

DISCUSSION: We hypothesized that S. aureus within the OLCN are less sensitive to the current revision and antibiotic therapies. By using a murine model of osteomyelitis and revision therapy, we conclude that standard of care antibiotics were not effective in reducing MSSA or MRSA bacterial load. These results could be due to the bacteria being within the OLCN were in a privileged environment, and therefore the antibiotics were unable to effectively eradicate the bacteria within the OLCN. TEM analysis of these bacteria will demonstrate the morphological effects of the antibiotics on the bacteria.

CLINICAL SIGNIFICANCE: Ultimately, these results lend new insight into S. aureus' unique pathogenicity in osteomyelitis, via deforming and elongating to invade the OLCN. These findings also challenge the clinical utility of these these commonly used antibiotics to eradicate implant-associated osteomyelitis

REFERENCES: 1) Nishitani, K. et al. J Orthop Res. 33, 1311-1319, (2015).

Title: **Endurance exercise rescues radiation-induced muscle dysfunction.**

Presenting Author: Thomas O'Connor

Co-Authors: Jacob Kallenbach, John Bachman, Nicole Paris, Romeo Blanc, Sundeep Malik, Linda Groom, Esraa Furati

Lab PI / Mentor: Joe Chakkalakal, Robert Dirksen

Abstract (3500 characters or 500 words Limit)

Exercise has several beneficial effects on overall health, such as increased bone strength and improved cardiovascular, cognitive, and immune system function. Similarly, exercise elicits improved muscle function by increasing muscle stem cell (satellite cell, SC) activation and improving excitation-contraction coupling through the establishment of Ca2+ Entry Units (CEUs) and upregulation of Ca2+ handling genes. However, radiotherapy, a mainstay in the treatment of many cancers, produces multiple adverse effects on skeletal muscle and has been shown to cause early-onset sarcopenia, a condition characterized by significant muscle weakening commonly observed in the elderly. Our studies show that radiation produces cytotoxic effects on SCs, depleting the SC pool and leaving the remaining SCs dysfunctional in their ability to activate and repair injured myofibers. We find that radiation exposure also alters expression of key Ca2+ handling genes in skeletal muscle including CASQ1, CACNB1, and CACNA1S which lead to altered resting Ca2+ levels and impaired excitation-contraction coupling. Aberrant expression of any of these proteins can also have significant effects on SR store Ca2+ levels, store-operated calcium entry (SOCE) efficiency, and mitochondrial function, impairing homeostatic oxidative phosphorylation and diminishing energy production required for muscle contraction.

Exercise inhibits radiation-induced sarcopenia and restores muscle function through several mechanisms. We hypothesize that exercise stimulates muscle regeneration and repair by activating the remaining SC pool. We also propose that exercise elicits restoration of homeostatic resting Ca2+ levels by upregulating integral Ca2+ handling genes such as CACNB1 and CACNA1S. Finally, we suspect that this restoration of proper Ca2+ kinetics directly improves mitochondrial function to support energy demands of the muscle, improving overall function.

Title: **Assessing the role of NF-kB repression during tendon healing**

Presenting Author: Meghan M. O'Neil

Co-Authors:

Lab PI / Mentor: Alayna E. Loiselle, PhD

Abstract (3500 characters or 500 words Limit)

Canonical NF-kB signaling is a proinflammatory pathway that drives both inflammatory and pro-survival gene expression. Canonical NF-kB signaling has been implicated both in acute and chronic tendon injuries. Previous work in the lab has explored the role of canonical NF-kB and ERK1/2 signaling activation via NFKB1 knock-out. The synergistic activation of NF-kB and ERK1/2 signaling resulted in an increase in ECM deposition during tendon healing. The goal of this study is to isolate the role of canonical NF-kB signaling in tendon cells. Previous studies have shown that global inhibition of canonical NF-kB signaling decreased scar tissue formation, decreased aSMA+ myofibroblast persistence, and decreased ECM production. p65 (Rel A) is directly responsible for initiating gene expression during NF-kB signaling as a heterodimer with p50. We hypothesize that knock-out of p65 in tendon cells will impair tendon healing due to the repression of NF-kB signaling that will prohibit persistence of aSMA+ myofibroblasts and F4/80+ macrophages, both of which drive scar tissue formation. We will utilize p65F/F mice crossed to Scx-CreERT2;Ai9 to inducibly delete p65 in Scleraxis positive tendon cells at different timepoints before injury and during healing. We plan to quantify knock-down efficiency, assess the biomechanical properties of p65KOScx tendons, and assess cell survival with a focus on myofibroblast persistence.

Title: **Semi-Randomized Zwitterionic Peptides Grant Anti-Fouling Behavior to Nanoparticles**

Presenting Author: Clyde Overby

Co-Authors: Jorge Jimenez, Baixue Xaio, Marian Ackun-Farmmer

Lab PI / Mentor: Danielle S.W. Benoit

Abstract (3500 characters or 500 words Limit)

Nanoparticles (NP) are a clinically proven siRNA delivery platform [1]. However, recent data indicate that NPs exhibit poor systemic delivery properties due to protein adsorption, which accelerates NP clearance via opsonization and macrophage uptake [2]. Anti-fouling NP surface modifications using poly(ethylene glycol) (PEG) and zwitterionic (ZI) polymers and peptides have been shown to be highly efficacious but are susceptible to immunological reactions due to consumer product overuse [2] and repeating molecular structures. As an alternative, we propose the use of semi-randomized ZI peptides (srZIPs) synthesized via controlled random substitution of similar amino acids (AAs) in a single sequence to produce libraries (10^3-10^6) of related peptides to modify NP. We hypothesize that srZIPs will provide anti-fouling characteristics to NP and also be immunologically unique, resisting adaptive immune reactions. To investigate these hypotheses, the design, synthesis, and characterization of srZIP-NPs in vitro and in vivo was explored.

Materials and Methods: A diblock copolymer comprised of a poly(dimethylaminoethyl methacrylate) (DMAEMA) first block and 25% DMAEMA, 50% butyl methacrylate, and 25% propylacrylic acid second block was synthesized via reversible addition fragmentation chain transfer (RAFT) polymerization, which spontaneously self-assemble into NPs in neutral aqueous conditions [3]. Peptide sequences were generated in silico and scored using an anti-fouling algorithm based upon a peptide-peptide interaction model (PASTA) [4]. Peptide sequences were scored to identify those with the lowest interaction potential (ΔG = 2.5 kJ/mol). 15 AA srZIPs were synthesized via solid phase peptide synthesis, with mixtures of multiple AA precursors for some syntheses to achieve semi-randomization. srZIP synthesis was confirmed through mass spectrometry and 1H-NMR. srZIP or 2 kDa PEG were conjugated to NP via carbodiimide chemistry srZIP-NP or PEG-NP controls. Conjugation was confirmed via the fluoraldehyde assay and NMR. NP aggregation was evaluated via dynamic light scattering (DLS) in the presence of serum and plasma, and adsorbed protein was quantified using the bicinchoninic acid assay. Macrophage uptake of NP was evaluated by flow cytometry and in vivo pharmacokinetics were characterized via intravital fluorescent microscopy of Cy7 labeled srZIP/PEG-NPs.

Results and Discussion: srZIP-NPs exhibit similar sizes to unconjugated NPs (~25 nm) in PBS. In serum and plasma, srZIP-NPs and PEG-NPs have a dramatic >14-fold reduced size compared with unmodified NPs, which undergo serum-mediated aggregation [5]. Serum protein adsorption to srZIP-NPs is reduced by 65% compared to unfunctionalized NP and 35% to PEG-NPs. Furthermore, srZIP-NPs uptake by macrophages is reduced by 30% compared to NPs and equivalent to PEG-NPs. srZIP-NPs circulation time increased 5-fold over NPs, exhibiting a half-life of 32 minutes.

Conclusions: Data suggest that srZIP functionalization bestows anti-fouling properties to NPs, reducing macrophage uptake and enhancing systemic circulation time. Future work will focus on evaluating in vivo biodistribution of and adaptive immune response to srZIP-NPs.

Refs: 1. David, A. et al. NEJM 379(1) (2018). 2. Verhoef, J.F., et al. Drug Discov. Today 19.12 (2014). 3. Convertine, A.J. & Benoit, D.S.W., et al. J. Control. Release 133.3 (2009). 4. Trovato, A., et al. PEDS 20.10 (2007). 5. Malcolm, D.W., et al. Bioeng transl med 1.2 (2016).

Title: **Absence of Thy1 Associated with Exacerbated Bone Loss Bone Loss, Increased Synovitis and Joint Damage in the TNF-transgenic (TNF-Tg) Mice Arthritis Model**

Presenting Author: Ananta Paine

Co-Authors: Ananta Paine, Maria de la Luz Garcia-Hernandez, Hengwei Zhang, H. Mark Kenney, Marc Nuzzo, Stacey Duemmel, Edward M. Schwarz, Lianping Xing, Christopher T. Ritchlin

Lab PI / Mentor: Christopher T. Ritchlin

Abstract (3500 characters or 500 words Limit)

Background/Purpose: Thy1 (CD90) is a glycosylated, glycophosphatidylinositol (GPI)-anchored membrane protein expressed on many cells, including T lymphocytes, stem cells, and fibroblasts. Thy1 is also abundantly expressed by mesenchymal stem cells (MSCs), and we previously demonstrated that it is required for osteoblast differentiation and bone homeostasis. The goal of this study was to examine if the knockout of the membrane protein Thy1 (CD90) is associated with increased pathologic bone resorption in a murine model of inflammatory arthritis.

Methods: We performed real-time PCR (RT-PCR) to compare Thy1 mRNA expression levels in mouse bone marrow cells and monocyte-derived dendritic cells (mDCs) of TNF overexpressing (TNF-Tg) and wild type (WT) mice and murine embryonic fibroblasts (MEFs) from (WT) mice. Subsequently, we also investigated the impact of the Thy1 deletion in TNF-Tg (Tg3647) mice, a murine model of inflammatory arthritis. To study the effect of Thy1 depletion on bone erosion, we analyzed bone loss by performing micro-computed tomography (micro-CT) analysis of the long bones and ankle joints of Thy1-/-TNF-Tg, TNF-Tg, Thy1-/- and WT mice. We also performed the histomorphometric analysis of hematoxylin and eosin (H&E)-stained tissue sections of the hind legs.

Results:In vitro assays revealed a significant decrease in Thy1 expression (40% - 65%) in primary bone marrow cells and mDCs of the TNF-Tg mice compared to the WT mice (Figure 1). Thy 1 mRNA levels decreased by more than 25% in murine embryonic fibroblasts following exposure to TNF for 24 hours. Most importantly, micro-CT analysis of the long bone and ankle joints revealed a significant increase in bone loss in the Thy1-/-TNF-Tg mice, compared to the TNF-Tg or Thy1-/- mice. In particular, a significant reduction in bone parameters was observed in Thy1-/- TNF-Tg mice compared to the TNF-Tg, Thy1-/-, or WT mice. Significant differences were noted in BV/TV (0.003 ± 0.02 in Thy1-/-TNF-Tg vs 0.024± 0.01 in TNF-Tg, $p < 0.01$, for tibia), trabecular number (1.57 ± 0.2 in Thy1-/-TNF-Tg vs 2.4 ± 0.1 in TNF-Tg, $p < 0.005$, for tibia), and trabecular thickness (0.026 ± 0.002 in Thy1-/-TNF-Tg vs 0.032 ± 0.01 in TNF-Tg, $p < 0.01$, for tibia). Similar bone loss was not noted in WT or Thy1 KO mice. Histomorphometric analysis of H&E-stained sections showed significantly increased peri-articular inflammation area and eroded articular surface in knee joints of Thy1-/-TNF-Tg mice compared to the TNF-Tg mice.

Conclusion: We find that Thy1 expression significantly decreased in MSCs and myeloid cells following exposure to TNF. The absence of Thy1 was associated with enhanced pathologic bone resorption, increased synovitis, and joint damage in the murine model of arthritis. Thus, TNF-mediated downregulation of Thy 1 may serve as an important mechanistic link between inflammation and progressive bone loss in inflammatory arthritis.

Title: **Efferocytosis by mesenchymal stromal cells induces senescence and disrupts mitochondrial and differentiation potential**

Presenting Author: Emily R. Quarato

Co-Authors: Allison J. Li, Yuko Kawano, Jane Zhang, Chen Yu, Charles O. Smith, and Roman Eliseev

Lab PI / Mentor: Laura M. Calvi

Abstract (3500 characters or 500 words Limit)

Mesenchymal stromal cell (MSC) dysfunction is implicated in multiple settings, including age-induced bone loss, radiation injury, and dysfunction of the hematopoietic stem cell niche in hematologic malignancies. Our laboratory studies the supporting role of MSCs and macrophages within the hematopoietic system and recently reported their role in the aged microenvironment. Aged marrow macrophages were found to be expanded but defective in their ability to phagocytose apoptotic cells (efferocytosis). MSCs have previously been reported to be facultative phagocytes during a period of embryonic development where macrophages are defective. We therefore hypothesized that MSCs possess an innate efferocytic capacity that, when active, impairs their differentiation capacity and other cellular functions. In vivo, we observed the phagocytic activity of MSCs through cell surface antigens and genetically in Nestin-GFP+ mice and quantified efferocytosis of fluorescently labeled apoptotic neutrophils to be 5%. Notably, phagocytic activity in MSCs was increased in aged mice and in a pre-leukemic murine model. Through in vitro assays utilizing a murine bone marrow stromal cell line (ST2), primary murine bone marrow stromal cells (mMSCs), and human bone marrow stromal cells (hMSCs) we analyzed the extent of efferocytosis in MSCs and determined the consequences to fate determination post an efferocytic event. We observed that 30% of MSCs actively conduct efferocytosis of senescent neutrophils in vitro in both ST2 and primary MSCs. In the MSCs that are actively engulfing, there was a significant increase to the rate of senescence and a decreased cellular proliferation count over controls and their non-engulfing counterparts. Likewise, we observed a global depression in differentiation potential to the osteoblastic and adipocytic lineages of MSCs that are actively engulfing over controls and their non-engulfing counterparts. As both efferocytosis and MSC differentiation are accompanied by changes in mitochondrial dynamics, we sought to determine if increased efferocytosis in MSC is associated with mitochondrial changes. Utilizing in vitro cultures of ST2 cells, MSCs' oxidative and glycolytic functions were observed to be globally decreased by MSCs that are actively engulfing over controls and their non-engulfing counterparts. Collectively, these data support that idea that efferocytic activity by MSCs compromises their function and fate determination, and is associated with disruption of mitochondrial activity. Therefore efferocytosis in MSCs may serve as a therapeutic target to mitigate MSC damage in the setting of aging, radiation and hematologic malignancies.

Title: **Early Complications and Reoperation Rates are Similar Amongst Open Reduction Internal Fixation, Intramedullary Nail, and Distal Femoral Replacement for Periprosthetic Distal Femur Fractures: a Systematic Review and Meta-Analysis**

Presenting Author: Gabriel Ramirez

Co-Authors: David Quinzi, Gabriel Ramirez, Nathan B Kaplan, Thomas G Myers, Caroline Thirukumaran, Benjamin F Ricciardi

Lab PI / Mentor: Caroline Thirukumaran

Abstract (3500 characters or 500 words Limit)

Periprosthetic supracondylar distal femur fracture (PPDFF) is one of the most common complications after total knee arthroplasty (TKA) with incidence rates of 0.3% to 3.5%. These fractures typically occur in an elderly, geriatric population and can have devastating consequences including loss of ambulatory status, perioperative morbidity, and mortality rates of up to 15% in the first year after surgery. Historical studies have reported poor outcomes with the use of non-operative management of these fractures, including the need for prolonged immobilization, and high rates of nonunion (40% of cases) and subsequent surgery (30% of cases). Due to the poor outcomes of conservative therapy, surgical fixation is the preferred management strategy, however, there is still considerable controversy regarding the optimal surgical procedure of choice.

Different methods of surgical fixation for PPDFF have received support in the past two decades, however, advances in implant technology have increased the focus on three primary treatments. These include open reduction internal fixation (ORIF) with periarticular locking plates, intramedullary nail fixation (IMN), or prosthetic replacement of the distal fragment with distal femoral replacement (DFR).

Though each surgical treatment has its advantages, considerable controversy remains regarding the surgical treatment of choice in acute PPDFF. Major limitations of existing literature include the predominant use of many smaller case series and a lack of comparative studies for the three techniques regarding reoperation rates and complications. Recent systematic reviews on PPDFF have either examined the outcomes of internal fixation techniques alone, prosthetic replacement alone, or combined internal fixation techniques to prosthetic replacement. There are no studies currently examining the complication rates and reoperation rates between the three techniques using a comprehensive systematic review and meta-analysis, and this may provide further insights into the surgical indications and future areas of study regarding surgical treatment of PPDFF.
The purpose of our study was to perform a systematic review and meta-analysis of existing literature to evaluate the early complication rates and revision rates of three types of treatment for PPDFF: 1) ORIF with periarticular locking plates, 2) retrograde IMN, and 3) prosthetic replacement using DFR. This is the first study to our knowledge to compare these three methods of fixation in a systematic review and meta-analysis with regards to complication rates and revision rates.

Title: Regulation of Mitochondrial Function by Manipulating Cyclophilin D Influences Osteogenesis and Bone Phenotype

Presenting Author: Rubens Sautchuk, Jr.
Co-Authors: Roman Eliseev
Lab PI / Mentor: Roman Eliseev

Abstract (3500 characters or 500 words Limit)

Bone health and maintenance are achieved by the appropriate balance between bone formation and bone resorption. During aging, osteoblast (OB) decreased activity, bone marrow stromal cell (BMSC) senescence and cellular pool exhaustion shift this tenuous balance in direction to the prevalence of bone resorption. Our lab and others have demonstrated that during OB lineage commitment, BMSCs must increase their use of OxPhos. However, higher OxPhos activity increases the probability of mitochondrial permeability transition pore (MPTP) opening due to higher levels of reactive oxygen species (ROS) and oxidative stress. MPTP opening is positively regulated by the mitochondrial matrix protein Cyclophilin D (CypD) and leads to loss of integrity of the inner mitochondrial membrane (membrane potential - $\Delta\psi m$) and of OxPhos function. Therefore, to maintain BMSCs committed to osteogenic lineage, MPTP inhibition is required to preserve $\Delta\psi m$, support OxPhos, and desensitize mitochondria to higher ROS levels. Our lab previously showed that CypD knock-out mice, a loss-of-function model of the MPTP, present with higher BMSCs' mitochondrial OxPhos function and osteogenicity and less osteoporosis burden. In contrast, CypD upregulation, as seen in aging, can permanently open the pore leading to mitochondrial dysfunction and bone loss. To investigate how CypD is regulated during OB differentiation, we measured CypD mRNA and protein expression in osteoinduced mouse BMSCs and found that it is downregulated during osteogenic differentiation. To characterize the effect of CypD regulation in OBs on bone development and maintenance we created an OB-specific CypD gain-of-function (GOF) mouse model expressing constitutively active CypD. As a proof of concept model, embryonically tamoxifen-induced 2.3kbCol1α1-CreERt2;caCypD newborn mice were analyzed for deficient bone formation using histology. Moving to a potential translational application of our findings, CypD GOF mice were used to mimic the higher MPTP activity seen in aging. Recombination was induced at 2 mo and samples collected at 4 and 12 mo. The effects of mitochondrial dysfunction were analyzed by in vivo imaging, metabolomics, histology, μCT, and biomechanical testing. In vitro data showed defective mitochondria presenting with lower $\Delta\psi m$ and decreased OB activity. Embryonically tamoxifen-induced newborn CypD GOF mice showed decreased bone and hypertrophic zone length for both humerus and femur. Adult mice collected at 4mo and 12mo presented decreased OB activity measured by in vivo imaging with BoneTag and via P1NP levels, decreased bone parameters measured by μCT analysis, and lower bone strength in biomechanical testing for both vertebrae and femur. Bone metabolomic analysis at 4mo revealed metabolic profile consistent with mitochondrial dysfunction and premature aging. Altogether, our data present strong evidence that CypD expression and mitochondrial function play a crucial role in regulating osteogenic signaling and bone health, and significantly enhance our knowledge on the interdependence of cell fate and bioenergetics.

Title: **NAD(P)H Autofluorescence Lifetime Imaging Enables Single Cell Analyses of Osteoblast Cellular Metabolism**

Presenting Author: Kevin Schilling Jr.

Co-Authors: Sergei Vinogradov, Edward Brown, and Xinping Zhang

Lab PI / Mentor: Xinping Zhang and Edward Brown

Abstract (3500 characters or 500 words Limit)

Energy metabolism plays an important role in osteoblast differentiation and bone mineralization. While a series of studies have suggested a role of glycolysis as a major metabolic pathway in osteoblast differentiation, studies measuring the energy consumption and mitochondria metabolism show that osteoblast differentiation coincides with the propagation of mitochondria and increased oxidative phosphorylation (OxPhos). It is unclear which energy pathway is mostly utilized by osteoblasts in vivo during repair as well as how the oxygen microenvironment could affect the metabolic state of osteoblasts which in turn impact differentiation and mineralization of bone forming cells. A novel, non-invasive, optical technique has been developed to obtain cellular metabolism information based on the intrinsic autofluorescence lifetimes of free and enzyme-bound NAD(P)H which reflect the metabolic state of single cells within the native microenvironment of the living tissue. The goal of our current study uses this technique, termed two-photon fluorescence lifetime microscopy (2P-FLIM), in conjunction with two-photon phosphorescence lifetime microscopy (2P-PLIM) with an established oxygen reporting nanoprobe, PtP-C343, to understand osteoblastic cellular metabolism and oxygen tension (pO2) at high spatial resolution in the context of normal bone tissue microenvironment. Prior to in vivo studies, NAD(P)H 2P-FLIM was initally performed in BMSC cultures established from bone marrow harvested from Col1 2.3GFP mice. GFP+ and GFP- cells were separately evaluated at week 2, 3, and 4 with or without osteogenic media. Measurement of the mean NAD(P)H lifetime, τM, demonstrated that cells in osteogenic media have a higher τM compared to cells in general media, indicating that more mature osteoblasts had increased OxPhos. Our data supported that as the osteoblast cells became more mature, they utilize relatively more OxPhos. In vivo NAD(P)H 2P-FLIM was conducted to evaluate cell metabolism in 1-2 month old native bone of Col1 2.3GFP mice. GFP+ cells residing in suture and bone marrow space, as well as cells embedded in bone lacunae were examined at the single cell level. τM was calculated for each cell and used to determine relative metabolism of glycolysis and OxPhos within labeled osteoblasts. It is evident that cells dwelling within lacunae had highest τM, indicating more usage of OxPhos as compared to osteoblasts at the bone edge of suture and bone marrow space. Measurement of pO2 in the same regions where NAD(P)H 2P-FLIM was performed showed that marrow space has lower pO2 than the nearby suture space as well as lacunae regions containing osteoblasts. Our data support that both glycolysis and OxPhos are being used in the osteoblasts with more mature osteoblasts utilizing more OxPhos in vitro and in vivo. By measuring cell metabolism and oxygen tension at the same location, our data suggest that cellular metabolism could be affected by the oxygen availability as well as the differentiation status of the osteoblasts. Further experiments utilizing animals with genetic modification of cellular metabolism will further enhance our understanding of energy embolism in cells at the various stages of differentiation.

Title: **Energy metabolism during osteogenic differentiation: the role of Akt**

Presenting Author: Charles Owen Smith

Co-Authors: Roman Eliseev

Lab PI / Mentor: Roman Eliseev

Abstract (3500 characters or 500 words Limit)

INTRODUCTION" Osteogenic differentiation, the process by which bone marrow mesenchymal stem/stromal (a.k.a. skeletal stem) cells and osteoprogenitors form osteoblasts, is a critical event for bone formation during development, fracture repair, and tissue maintenance. Extra- and intracellular signaling pathways triggering osteogenic differentiation are relatively well known; however, the ensuing change in cell energy metabolism is less clearly defined. We and others have previously reported activation of mitochondria during osteogenic differentiation. To further elucidate the involved bioenergetic mechanisms and triggers, we tested the effect of osteogenic media containing ascorbate and β-glycerol phosphate, or various osteogenic hormones and growth factors on energy metabolism in long bone (ST2)- and calvarial bone (MC3T3-E1)-derived osteoprogenitors.
METHODS: We performed bioenergetic pathway analysis of cells using the Seahorse Flux Analyzer and confirmed osteogenic potential using a combination of alkaline phosphatase, quantitative PCR, and western blotting.
RESULTS: We show that osteogenic media, and differentiation factors, Wnt3a and BMP2, stimulate mitochondrial oxidative phosphorylation (OxPhos) with little effect on glycolysis. The activation of OxPhos occurs acutely, suggesting a metabolic signaling change rather than protein expression change. To this end, we found that the observed mitochondrial activation is Akt-dependent. Akt is activated by osteogenic media, Wnt3a, and BMP2, leading to increased phosphorylation of various mitochondrial Akt targets, a phenomenon known to stimulate OxPhos.
DISCUSSION: In sum, our data provide comprehensive analysis of cellular bioenergetics during osteoinduction in cells of two different origins (mesenchyme vs neural crest) and identify Wnt3a and BMP2 as physiological stimulators of mitochondrial respiration via Akt activation.

Title: **Talocalcaneal interosseous ligament provides greatest talar stability in the sagittal plane**

Presenting Author: Michelle L. Smith, MS, MD

Co-Authors: Emma Knapp, BS, Hani A. Awad, PhD, and Irvin Oh, MD

Lab PI / Mentor: Irvin Oh, MD

Abstract (3500 characters or 500 words Limit)

Talar AVN, trauma, and implant failure or body collapse after total ankle replacement are becoming major challenges in foot and ankle surgery. Custom total talar implants are a promising option for such conditions, especially in a young and active patient population. However, there has been no biomechanical studies examining the peritalar kinematics of total talus implant. We aimed to investigate the most critical stabilizers of the native talus and the biomechanics of a total talar replacement . We hypothesize that the stability a total talus implant is less affected by medial and lateral ligaments as partial stability is provided by the mortise of the ankle joint and the most instability is noted on the talo-calcaneal joint due to the absence of plantar restraint. Total talar implant will be most unstable in the sagittal plane, especially in heel-raise position.

Testing was performed on 8 cadaveric samples which underwent biomechanical testing in a midstance model and seated heel-raise model (30□ plantar flexion) using custom jigs fixed to an E10000 Instron system. 3D motion sensors were placed in the tibia, talus, calcaneus, navicular and first metatarsus. Cameras captured the 3D positions of the markers throughout testing. In the midstance model, the Achilles tendon was loaded in tension while the tibia was cyclically loaded to create an 800N ground force reaction force. In the seated heel raise model, the sample was placed in 30□ of plantar flexion and the Achilles tendon was loaded while the tibia was cyclically loaded to create a 200N ground reaction force. The antero- and posterolateral ligaments were released and underwent 25 cycles in midstance and heel-raise positions. This was repeated for the following ligament releases: deep deltoid ligaments, talonavicular joint capsule, and the talo-calcaneal interosseous ligament. The talus was completely removed from the joint and placed back to simulate total talar implant. Lastly, TA, EHL, and EDL were sutured back into place to provide static soft tissue coverage of the talus, and final kinematics were measured. Data was analyzed to determine the joint motion and joint angles under maximum load. Releases were compared using a one-way ANOVA, and compared to the initial condition using a one-sample t-test.

Under maximum force in a seated heel-raise position, there is a significant difference in sagittal angle of the talus relative to the navicular ($p = 0.0314$, 0.0055, and 0.013 for the deep deltoid ligaments, talonavicular joint capsule, and TCIL releases, respectively). There is also significant difference in the total displacement of the talus relative to the navicular ($p = 0.0263$, 0.0105 for talonavicular joint capsule and TCIL releases, respectively). These changes are compared to the initial condition. These changes are most pronounced after the TCIL release.

In this study, we utilized native talus as a surrogate for a custom total talar implant to investigate the peritalar kinematics of the total talus implant. We found that the TCIL provides the most talar stability in the native ankle joint. Without the TCIL, the talus is most unstable in the sagittal plane, especially during the heel raise position. A significant medial and lateral stability of the tibiotalar joint maybe provided by the mortise of the ankle joint. Taken together, recreation of the TCIL or plantar stabilization of the implant should be considered to improve stability of a total talar implant.

Title: **Recruitment and Differentiation of Leukemia-Associated Macrophages**

Presenting Author: Celia Soto

Co-Authors: Maggie Lesch, Joshua C. Munger, Ph.D.

Lab PI / Mentor: Benjamin J. Frisch, Ph.D.

Abstract (3500 characters or 500 words Limit)

The bone marrow microenvironment provides signals to hematopoeitic stem cells (HSCs) that are vital to maintain their self-renewal and differentiation. In leukemia, there is disruption of the bone marrow microenvironment leading to further dysregulation of normal hematopoiesis. Leukemia-associated macrophages (LAMs) have an alternative activation profile from classically activated macrophages, although little is known mechanistically about how marrow macrophages are recruited, and alternatively activated during leukemia. Current literature reports that in solid tumors the microenvironment polarizes macrophages to a tumor-associated macrophage (TAM), similar to a M2-like phenotype, that supports cancer cell survival, and that elevated levels of the secreted chemokine CCL3 recruits monocytes from circulation to the tumors. Our laboratory previously reported that CCL3 is overexpressed in myeloid malignancies, and is required for homeostatic myeloid differentiation and hematopoietic stem and progenitor cell maintenance in both normal hematopoiesis and leukemic development. CCL3 also mediates the recruitment of monocytes and macrophages in the hematopoietic tumor Multiple Myeloma. Because of its potential use as a therapeutic target, the mechanisms by which CCL3 affects the bone marrow microenvironment is an ongoing topic for study.

Cancer cells in solid tumors have been shown to switch their metabolic state to preferentially perform aerobic glycolysis even in hypoxic conditions (Warburg effect), which produces lactic acid. Similarly, leukemic cells are dependent on aerobic glycolysis, resulting in increased lactic acid production. We have demonstrated through flow cytometric analysis that bone marrow macrophages in leukemic mice express higher levels of the M1 marker MHCII and the M2 marker CD206, both of which have previously been reported as overexpressed in TAMs. In vitro treatment of primary bone marrow macrophages with lactic acid recapitulated the increased CD206 expression, suggesting lactic acid in the bone marrow microenvironment as a mechanism of LAM polarization. We and others have previously reported that osteoblastic dysfunction is a key feature of the leukemic bone marrow. In vitro exposure of primary bone marrow mesenchymal stem cells (MSCs) to lactic acid decreased their proliferation, and decreased their capability to differentiate into mature osteoblastic cells, as measured by CFU-OB assays.

Future directions of this research aim to profile the metabolic landscape of leukemic marrow in mouse and human AML patient bone marrow plasma samples through LC/MS/MS metabolomics studies. We hypothesize that CCL3 overexpression in leukemic marrow recruits monocytes from circulation, and that the increased lactic acid levels in the bone marrow polarize macrophages to an alternatively activated LAM phenotype, driving bone marrow dysfunction.

Title: **Peritalar Kinematics Restored with Combined Subtalar Fusion and Medial Ligament Reconstruction in a Simulated Advance Adult Acquired Flatfoot Deformity Model**

Presenting Author: Nahom Tecle

Co-Authors: Emma Gira, Hani Awad, Irvin Oh

Lab PI / Mentor: Irvin Oh

Abstract (3500 characters or 500 words Limit)

INTRODUCTION:
Advanced adult acquired flatfoot deformity (AAFD) may lead to a disruption of the medial peritalar ligaments, including the spring and deltoid ligaments, with progressive loss of the medial arch and further valgus alignment of the subtalar and tibiotalar joints. This ultimately leads to peritalar instability and degenerative osteoarthritis of the subtalar and tibiotalar joints. Some authors have suggested subtalar fusion (SF) with or without MCO as an alternative option. Although SF may provide a more effective correction, a resultant increase in valgus moment arm due to a larger strain on the medial ankle ligament has been reported. The aim of our study is to investigate the efficacy of a combined MCO with SF and medial tibionavicular ligament (TNL) reconstruction on restoring peritalar stability. A secondary aim was to determine if a tibiocalcaneonavicular ligament (TCNL) reconstruction would provide comparable peritalar stability.

METHODS:
Ten fresh-frozen cadaveric foot specimens were employed to create a severe AAFD model. Reflective markers were placed on the tibia, talus, navicular, calcaneus, and first metatarsal. A multiple-camera motion capture system was utilized to document peritalar joint kinematics (OptiTrack, Prime13). Severe AAFD model was created by sectioning the medial capsuloligamentous complex followed by cyclic axial loading. Sequential surgical procedures were completed, including MCO, SF, MCO + SF, MCO + SF + medial tibionavicular ligament (TNL) reconstruction, and MCO + TCNL repair. Subtalar joint coronal angle, tibiotalar coronal angle, forefoot abduction axial angle, and talo-first metatarsus (Meary's) lateral angle were calculated for each sequential procedure and compared to the severe flatfoot model. The kinematic changes were calculated between groups utilizing a custom MatLab code and statistical significance was determined using a one-way ANOVA and a Tukey's multiple comparison test (GraphPad Prism, San Diego, CA).

RESULTS:
The subtalar joint valgus angle of the severe AAFD model (mean XX°) was significantly reduced by the MCO+SF+TNL reconstruction (mean X, p = 0.00X) and MCO + TCNL reconstruction (mean Y, P= 0.0253). The tibiotalar joint valgus angle of the severe flatfoot model (mean YY°) was reduced after the MCO+SF+TNL reconstruction (mean ZZ°, P= 0.0273) and after the MCO + TCNL (mean AA°, P= 0.0471). Forefoot abduction angle was found to be significantly reduced in all reconstruction methods compared to the severe flatfoot model. Meary's angle was also significantly reduced after the MCO+SF+TNL reconstruction (P= 0.0084) and MCO + TCNL reconstruction (P= 0.0019).

DISCUSSION:
MCO+SF+TNL reconstruction most effectively corrected kinematic derangement of a severe AAFD in our cadaveric model. Restoration of peritalar stability was reflected by significantly improved subtalar, tibiotalar, forefoot abduction, and Meary's angles. The addition of a TCNL reconstruction to MCO also improved the subtalar joint valgus angle. MCO+SF+TNL reconstruction or combined deltoid-spring ligament (TCNL) reconstruction maybe considered in advanced AAFD.

Title: **Targeting of Bone Marrow Using Tartrate-Resistant Acid Phosphatase (TRAP)-binding Peptide Functionalized Nanoparticles (TBP-NP)**

Presenting Author: Baixue Xiao

Co-Authors: Marian Ackun-Farmmer

Lab PI / Mentor: Danielle Benoit

Abstract (3500 characters or 500 words Limit)

Bone marrow (BM) is the major organ of the hematopoietic system and is implicated in multiple cancers including acute and chronic leukemia, multiple myeloma, myelodysplastic syndrome and bone metastases from solid tumors. Effective therapeutic doses for treatment of cancers is difficult upon systemic administration of drugs, which results in high rates of relapse as well as serious side effects. Limitations in current treatments motivate the development of bone marrow targeted drug delivery systems to enhance drug targeting and minimize dose-associated adverse effects. We have previously developed a bone-targeted nanoparticle (NP) drug delivery system (DDS). This DDS is comprised of self-assembled diblock copolymers of poly(styrene-alt-maleic anhydride)-b-poly(styrene) (PSMA-b-PS). Targeting is achieved via incorporation of peptides with subnanomolar affinity to tartrate resistant-acid phosphatase (TRAP), a bone-specific enzyme deposited by osteoclasts during bone remodeling. Our previous studies using TRAP-binding peptide-targeted NP (TBP-NP) to deliver a small molecule Wnt agonist revealed enhanced bone regeneration owing to robust ~6-fold accumulation to femur fractures compared to controls. Interestingly, 4-fold accumulation of TBP-NP was also observed in contralateral marrow. Based on these remarkable findings, we sought to investigate the mechanism of TBP-NP accumulation within marrow. Specifically, the relationship between TRAP deposition and accumulation of TBP-NP was studied using two murine models, which exhibit transient TRAP upregulation. Specifically, mice in which blast crisis chronic myeloid leukemia (bcCML) was induced, which serves as a relevant disease model, and those fed a low calcium diet. In the bcCML model, there was a 1.4-fold increase in BM accumulation of TBP-NP compared to untargeted NP. Furthermore, in mice fed a low calcium diet, increased TRAP deposition was associated with a 1.7-fold increase in BM accumulation of TBP-NP. In future studies, the strain and sex-dependent effects of NP marrow accumulation will be investigated and evaluation of TRAP and TBP-NP colocalization using immunohistochemistry. Altogether, these studies demonstrated robust bone marrow accumulation through TBP-NP-TRAP interactions, which have widespread applicability in myriad hematopoietic and orthopaedic diseases to realize enhanced target efficiency and minimal side-effects.

Title: **3D Printable PCL Scaffolds Containing Carboxymethyl Chitosan and Amorphous Calcium Phosphate Nanoparticles for Infected Bone Repair**

Presenting Author: Ming Yan

Co-Authors: Edward Schwarz

Lab PI / Mentor: Hani Awad

Abstract (3500 characters or 500 words Limit)

The standard clinical treatment of device-related osteomyelitis (OM) involves multiple surgeries which include systemic antibiotics, a thorough debridement of the infected bone and soft tissue, the implantation of a temporary antibiotic-laden poly(methyl methacrylate) (PMMA) bone cement spacer to treat the infection, removal of the PMMA spacer, and the implantation of new hardware and reconstruction of the missing bone. Clinical and experimental data show that most bone cements have limited drug delivery (5-15% of drug payload) in burst release profiles over 24-48 hours. Therefore, there is debate on whether these antibiotic spacers are effective. Moreover, clinical data and our own experiments in mice have shown that the surfaces of these antibiotic spacers become colonized with biofilm. To address this, we previously showed in mouse models of established OM that 3D printed polymer (PLGA) and calcium phosphate (CaP) scaffolds are more effective than PMMA for localized delivery of antibiotics. However, these scaffolds were brittle and lacked innate osteoinductive properties, rendering their effectiveness in single-stage reconstruction surgeries questionable. Studies in the dental field have shown that carboxymethyl chitosan (CMC) amorphous calcium phosphate (ACP) nanoparticles (CANP) can effectively inhibit bacterial adhesion and promote biomineralization4. Previous studies showed that during osteogenesis, osteoblasts secrete vesicles containing ACP which infiltrate the organized collagen fibers, and begin to mineralize by forming hydroxyapatite (HA). The transformation of ACP to bone-like apatite in soft nanofibrous polymeric matrices has been described, and led to mechanistic insights about engineered biomineralization. To test the hypothesis that the antimicrobial properties of CMC and the osteoinductive properties ACP can be harnessed in 3D printed polycaprolactone (PCL) scaffolds for single stage management and repair of infected bone, we developed an extrusion-based 3D-printable hyperelastic PCL:CANP bioink. Using this system, we evaluated the physical and chemical characteristics, the cytocompatibility, and antimicrobial properties of 3D printed PCL:CANP scaffolds in vitro. Using FTIR, we comparted the spectra of CMC, ACP, CaP, and CMC/ACP. The spectra showed the characteristic peaks of ACP and CMC in the individual compositions and CANP, and were distinct from the spectra of CaP. The X-ray scattering curves for the ACP and CANP lacked the characteristic peaks of CaP, suggesting that the ACP in the CANP maintains its amorphous, non-crystalline state. The size distribution of the CANP was analyzed by DLS, which averaged 236nm with a polydispersity index of 0.196. The printed PCL:CANP scaffolds maintained a structure consistent with the digital design and SEM imaging showed the exposure of nano-scale microstructure of the CANP on the surface of the PCL lattice. ST2 cells-seeded PCL:CANP scaffolds showed greater than 95% viability, and were comparable to PCL only scaffolds. Compared to PCL scaffolds, PCL:CANP scaffolds showed significantly reduced bacterial colonization. Thus, our results show that 3D printed PCL:CANP scaffolds maintain the osteogenic amorphous state of ACP and antibacterial properties of CMC and display excellent cytocompatibility and resistance to bacterial colonization. Future studies will evaluate the antimicrobial and osteoinductive properties of the 3D printed PCL:CANP in our established mouse models of OM.

Title: **Targeted radiation evokes catecholamine production triggering rapid inflammatory responses**

Presenting Author: Yuko kawano

Co-Authors: Daniel K. Byun, Hiroki Kawano, Mark W. Lamere, Lizz Lamere, Carl J. Johnston, Jacqueline P. Williams

Lab PI / Mentor: Laura M. Calvi

Abstract (3500 characters or 500 words Limit)

Targeted irradiation (TR) is widely used for tumor treatment in the clinic. Even though TR has a lot of benefits for tumor therapy, it is known to have general adverse effects such as myeloablation and secondary malignancies. Recent studies suggest that the innate and acquired immune systems response to radiation not only contribute to elimination of tumor cells or dead cells, but at the same time also cause prolonged tissue injury that may result in the generation of secondary malignancies. To elucidate the mechanisms underlying these general adverse effects of TR, we utilized a murine model using small animal radiation research platform (SARRP). With SARRP, we targeted one side tibia of 6-8 weeks old B6 mice by single dose of 15Gy radiation, and analyzed both radiated side (TR), and contralateral side (Cont). We found that multiple inflammatory cytokines and chemokines, such as IL-1b, IL-18, CCL2, CCL3, CXCL2, CXCL9, CXCL10 were upregulated from very early phase (2hrs) up to 48hrs in the bone marrow extracellular fluid (BMEF) of the radiated tibiae. Consistent with dynamics of these cytokines, we observed influx of myeloid cells and expansion of T cells peaking at 6hrs in bone marrow (BM) . At the same time of these immune responses Norepinephrine (NE) was elevated in BMEF. Since recent studies showed that the catecholamine production from myeloid cells may augment cytokine production in the setting of viral infection and immunotherapy, we hypothesized that BM myeloid cells respond to radiation-induced cell damage by producing catecholamines that may then trigger a systemic inflammatory response after radiation. To begin to test this hypothesis, we utilized standard long-term bone marrow cultures (M-LT-BM) thatreproduce three-dimensional BM structures with myeloid-skewed condition in vitro, and directly irradiated it to look at inflammatory changes induced by radiation at 2, 6 and 24hrs. In this experimental model, 5Gy of direct radiation led to the elevation of catecholamines along with the production of chemokines like CXCL2, CXCL9 mostly peaking at 6hrs in the cell culture supernatants . These data demonstrate that, in response to radiation, there is local bone marrow production of catecholamines that does not depend on systemic innervation. Further studies are needed to identify the population of cells responsible for catecholamine production, and whether catecholamines regulate chemokines in response to irradiation. Therefore, inhibition of catecholamine production in the BM could be novel therapeutic tool to prevent adverse effect of TR.


1850
MELIORA
UR
MEDICINE